Quantum anomalous Hall effect for metrology

Nathaniel J. Huáng, ^{1, a)} Jessica L. Boland, ^{1, 2, b)} Kajetan M. Fijalkowski, ^{3, c)} Charles Gould, ^{3, d)} Thorsten Hesjedal, ^{4, e)} Olga Kazakova, ^{1, 5, f)} Susmit Kumar, ^{6, g)} and Hansjörg Scherer^{7, h)}

United Kingdom

(Dated: 15 January 2025)

The quantum anomalous Hall effect (QAHE) in magnetic topological insulators offers great potential to revolutionize quantum electrical metrology by establishing primary resistance standards operating at zero external magnetic field and realizing a universal "quantum electrical metrology toolbox" that can perform quantum resistance, voltage and current metrology in a single instrument. To realize such promise, significant progress is still required to address materials and metrological challenges – among which, one main challenge is to make the bulk of the topological insulator sufficiently insulating to improve the robustness of resistance quantization. In this *Perspective*, we present an overview of the QAHE; discuss the aspects of topological material growth and characterization; and present a path towards a QAHE resistance standard realized in magnetically doped (Bi,Sb)₂Te₃ systems. We also present guidelines and methodologies for QAHE resistance metrology, its main limitations and challenges as well as modern strategies to overcome them.

I. INTRODUCTION

Electrical metrology is a domain that has been at the forefront of adopting new physics. Discovered more than a century ago¹, the Hall effect underwent a transformative evolution when Klaus von Klitzing observed its quantized counterpart in 1980 in a two-dimensional electron gas system (2DES). This discovery of the quantum Hall effect (QHE)² linked the Hall resistance R_H to universal SI constants³ – Planck's constant (h) and electron charge (e), with the von Klitzing constant R_K defined as $R_H = \frac{R_K}{i} = \frac{h}{ie^2}$, where i is an integer). This revolutionized resistance metrology by establishing the QHE as the primary resistance standard (PRS). Currently, high-quality 2DES to observe QHE are fabricated in GaAs/AlGaAs quantum well heterostructures grown by molecular beam epitaxy (MBE). Graphene, a twodimensional single atomic layer of carbon, was quickly realized as promising PRS after its discovery^{4,5}. Over the years, the metrology community has refined the production of epitaxial graphene and developed fabrication techniques suitable for resistance standards. Graphene devices have

The grand goal of electrical metrology is to realize a "quantum electrical metrology toolbox" where the three components of the quantum electrical metrology triangle – the volt (V), ampere (A), and ohm (Ω) – exist in a single system. To achieve this, a "relaxed-condition" environment (including zero-to-low magnetic fields, higher operation temperatures and currents, and the ability to fabricate large-area devices⁷) is critical for universal adoption of quantum electrical SI standards from metrological laboratories to industry. The quantum anomalous Hall effect (QAHE) intrinsically offers a path to circumvent the necessity to form Landau levels to realize a PRS with unsurpassed accuracy in such "relaxed conditions". This Perspective presents recent advancement and current challenges for the realization of QAHE-based PRS, and provides strategies and methodologies towards a new era of quantum electrical metrology.

a) All authors contributed equally. Author to whom correspondence may be addressed: nathaniel.huang@npl.co.uk.

II. QUANTUM ANOMALOUS HALL EFFECT

A. Overview

The idea of the QAHE dates back to 2003 and was first discussed in the context of 2D ferromagnets⁸. The breakthrough came with the advent of topological insulators (TI)^{9–17}, where the QAHE was first predicted to emerge in (Hg,Mn)Te quantum wells¹⁸. There, the magnetic exchange interaction from

¹⁾Department of Quantum Technologies, National Physical Laboratory, Teddington TW11 0LW, United Kingdom

²⁾Photon Science Institute and Department of Materials, University of Manchester, Manchester M13 9PL, United Kingdom

³⁾Institute for Topological Insulators and Faculty for Physics and Astronomy (EP3), Universität Würzburg, 97074 Würzburg, Germany

⁴⁾Department of Physics, Clarendon Laboratory, University of Oxford, Oxford OX1 3PU,

⁵⁾Department of Electrical and Electronic Engineering, University of Manchester, Manchester M13 9PL, United Kingdom

⁶⁾ Justervesenet - Norwegian Metrology Service, 2007 Kjeller, Norway

⁷⁾Physikalisch-Technische Bundesanstalt, 38116 Braunschweig, Germany

shown remarkable agreement with the GaAs resistance standard maintained by the International Bureau of Weights and Measures, with a variance within $1 \text{ n}\Omega/\Omega$ and an uncertainty of $\pm 3 \text{ n}\Omega/\Omega^6$.

b) jessica.boland@manchester.ac.uk

c) kajetan.fijalkowski@physik.uni-wuerzburg.de

d) charles.gould@physik.uni-wuerzburg.de

e)thorsten.hesjedal@physics.ox.ac.uk

f)olga.kazakova@npl.co.uk

g)sku@justervesenet.no

h)hansjoerg.scherer@ptb.de

the Mn atoms lifts the band inversion for one of the two spin species, effectively "removing" one of the two helical edge modes of the quantum spin Hall effect (QSHE)^{9-11,15,19}. A remaining single chiral edge mode is a realization of the QAHE with a Chern number C = 1. (Hg,Mn)Te is paramagnetic²⁰, which prevents it from realizing electronic quantization at zero external magnetic field²¹. Fortunately, another material family emerged: group V-VI ferromagnetic TIs (transition metal doped Bi₂Te₃, Sb₂Te₃, and Bi₂Se₃)^{22,23}, followed by a long-awaited experimental realization of the zero external magnetic field QAHE in Cr-doped (Bi,Sb)₂Te₃ (BST) in 2013²⁴, soon afterwards reproduced by multiple independent groups^{25–31}. Most notably, despite all the progress in the field, metrologically relevant precision of QAHE quantization has thus far been only reported in Cr/V-doped (Bi,Sb)₂Te₃^{7,32–36}. A key point to appreciate is that the difficulty in achieving a pristine QAHE in a TI lies in controlling the bulk insulator rather than the topological surface state. The topological state is robust to perturbation. The bulk however is not protected and, given the relatively narrow band gaps which are ubiquitous in TIs, is very challenging to make sufficiently insulating. For a comprehensive understanding of the physical mechanisms, relevant material systems, and potential applications of the QAHE, the reader is referred to a recent review³⁷ by Chang et al.

B. Dimensionality and axion electrodynamics

The original idea for realizing the QAHE from "removing" one of the two QSHE edge modes of a two-dimensional TI¹⁸ implies that the effect is inherently two-dimensional. Indeed, the conductivity tensor $(\sigma_{xx}, \sigma_{xy})$ scaling behavior analysis of the QAHE films^{25,38–40} often reveal symmetries concurrent to that of conventional OHE observed in ordinary 2DESs^{41–46}, without any non-trivial electrodynamics⁴⁷. On the other hand, a perspective of the QAHE from the surface state of a threedimensional TI film paints a more intriguing picture and involves axion electrodynamics^{48–54}. Axionic corrections to Maxwell's equations lead to a half-integer $\sigma_{xy} = \frac{e^2}{2h}$ quantization of Hall conductance from an individual topological surface^{49,52-56}, and a signature of such half-integer quantization can be regarded as evidence for axion physics. This quantization has recently been extensively studied and debated in various electronic transport^{47,57–64} and optical^{65–68} experiments. Noteworthy, an apparent distinct QAHE origin in two- and three-dimensional magnetic TIs implies a distinct protection mechanism for a topological state in each, potentially carrying relevance for practical applications.

C. Unusual magnetism

The nature of interactions underpinning the magnetism remains an open question. Cr- and V-doped $(Bi,Sb)_2Te_3$ materials have similar Curie temperatures ~ 20 K but vastly different strength of magnetic anisotropy^{24,30}. Various

mechanisms were attempted to explain experimental observations, including Van Vleck ferromagnetism^{23,24,69–72}, Ruderman-Kittel-Kasuya-Yosida interactions^{69,72,73}, and double-exchange/superexchange mechanisms^{74–77}. While it appears that ferromagnetism plays an important role^{24,30,72}. there is evidence for superparamagnetic-like dynamics⁷⁸, even concurrent with perfect electronic transport quantization near zero external magnetic field³¹. Electronic transport studies reveal rich magnetic domain driven phenomenology^{79–81} when the device size approaches a characteristic magnetic domain dimension^{72,78,82,83}. Individual magnetic domains can have a ground state with magnetization pointing antiparallel relative to its neighbors⁸⁰, indicating a complex competition of ferro- and antiferromagnetic domain-domain interactions. In addition, other complex magnetic phenomena were reported on in this material system, including magnetic skyrmions^{84–86}, coexistence of surface and bulk ferromagnetism 87 , adiabatic cooling 27 , sizable Barkhausen-like switching 88 , and macroscopic quantum tunneling of the magnetization⁸⁰. It is not yet clear how all the experimental observations can be reconciled within a single unified model.

D. Operational parameter space and experimental limitations

The stability of QAHE in Cr/V-doped (Bi,Sb)₂Te₃ has been studied in detail. The explored parameter space includes the measurement current $^{33,89-92}$, temperature $^{24,29,30,93-95}$, material composition $^{96-98}$, and layer thickness 47,63,99,100 . The effect turns out to be surprisingly fragile, operating only in a narrow experimental window. Specifically to temperature, despite recent progress in increasing the operational temperature to $\sim 1 \text{ K}^{96,98,101}$, a regime of metrologically relevant quantization remains limited to the mK range^{7,32–36}. The exact mechanism limiting the QAHE temperature is not yet fully understood, but it is likely to be related to formation of charge puddles^{91,102–106} from material composition fluctuations, as the material is a mixed compound of n-type Bi₂Te₃ and ptype Sb₂Te₃¹⁰⁷. The concentration of magnetic doping can also fluctuate within the layer, which in addition to introducing magnetic inhomogeneities, can contribute to charge puddle formation if the magnetic dopants do not incorporate isoelectrically into the lattice. While the impact of these inhomogeneities can likely be reduced by further MBE development, the existence of charge puddles appears to be unavoidable due to inherently narrow bandgaps ubiquitous to TIs. Indeed, even state-of-the-art crystalline quality zinc-blende topological materials, such as HgTe, suffer from charge puddles affecting the electrical transport ^{108,109}, despite more than 40 years of MBE growth development 110 and 60 years of overall materials development¹¹¹. The position of the bulk valence band maximum in the band structure relative to the Fermi level could also play an important role⁹³. In terms of the quality of QAHE quantization, the key parameter that needs to be optimized is the resistivity of the material between the edge channels⁹⁵. The reports of edge state transport persisting up to the bulk Curie temperature ^{29,94,95} imply that the topological state itself is robust, thus, further improvements are possible through materials optimization. For completeness we also mention that there has been some literature questioning the validity of a pure edge state description of the transport 112,113, but in the end, as long as the Hall resistance can be optimized close enough to perfect quantization, the effect can be used for metrology, regardless of the microscopic details of the current distribution within the device. On the issue of measurement current, the primary breakdown mechanism stems from the Hall electric field build-up when current is increased^{33,89–92}. The build-up drives backscattering through the bulk and hinders the quantization. Recently, a new measurement scheme, "balanced quantum Hall resistor", aimed at eliminating this electric field has been demonstrated 92,114. Currently the metrology-grade experiments at zero external magnetic field remain limited to currents <100 nA^{32–36}. Application of an external magnetic field improves this to about 1 μ A⁷. Given that integer QHE based resistance standards routinely operate at currents >10 μ A¹¹⁵, significant improvements of QAHE performance are necessary.

E. Thin film growth

The Cr/V-doped (Bi,Sb)₂Te₃ thin films have been successfully grown using MBE on a wide variety of single-crystalline substrates, e.g., Al_2O_3 (0001)^{116–120}, $SrTiO_3$ (111)^{121,122}, GaAs (111)^{123–126}, Ge (111)^{127,128}, Si (111)^{129–134} (Figure 1), CdS (0001)¹³⁵, and graphene¹³⁶. The lattice mismatch for TI films on these substrates is large, reaching ${\sim}40\%$ for graphene¹³⁷. In fact, the governing van der Waals epitaxy growth mechanism does not require a perfect lattice match between film and substrate ^{138,139}. The absence of strong ionic or covalent bonding across the film-substrate interface unavoidably results in some loss of control over the growth. The grains originating from randomly dispersed nucleation centers coalesce and form defects at their boundaries. For example, films on c-plane sapphire are known to exhibit rotational twins, i.e., 6-fold symmetric reflection high-energy electron diffraction (RHEED) patterns, representative of the $R\bar{3}m$ crystal structure. In contrast, films grown on BaF2 (111) are twinfree¹⁴⁰. In general, the transport properties of TI films are most commonly not heavily dependent on the choice of substrate, but strongly affected by the generally large defect density at the interface¹⁴¹.

The deposition technique of choice for TI thin films is MBE. The growth of (Bi,Sb)₂Te₃ thin films by MBE is usually carried out with a considerable chalcogen overpressure on the order of 10:1 due to the high probability of re-evaporation ¹⁴², which can be lower if a chalcogen cracker cell is employed ¹⁴³. The growth rate is absorption controlled via the group-V element flux. The substrate temperature is the key parameter for controlling the film quality ¹³⁷, which can be optimized further employing a two-step growth recipe, whereby a seed layer is first grown at a lower temperature ¹¹⁹. Compensation doping has proven to be a successful strategy in electrically controlling defects. While Bi₂Te₃ can either be *n*- or *p*-type due to its ability to easily form both antisite defects and Te vacancies, Sb₂Te₃ is exclusively *p*-type due to its inclination

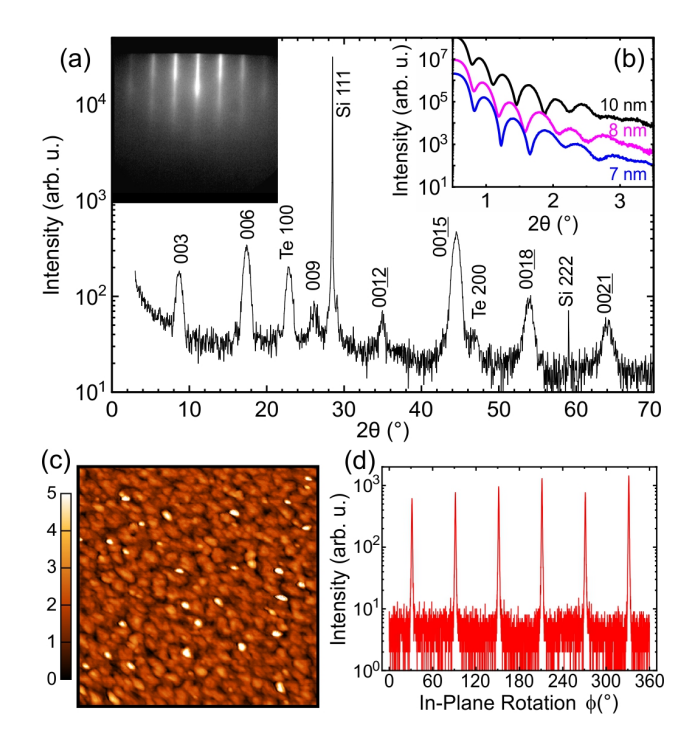


FIG. 1. (a) XRD θ -2 θ scans of a V_{0.1}(Bi_{0.21}Sb_{0.79})_{1.9}Te₃ film on Si (111). The film is 9 nm in thickness and capped with a 10-nm-thick Te layer to prevent the film from oxidation. The inset on the left depicts a RHEED pattern obtained from a similar layer's surface. (b) XRR profiles for similar layers measuring 7 nm (blue), 8 nm (magenta), and 10 nm (black) in thickness, displayed with sequential offsets of a factor of 10 for visual clarity. (c) $2 \times 2 \mu m^2$ AFM scan (5 nm z-scale) of an uncapped, 10-nm-thick film. (d) ϕ scan of {015} reflections demonstrating the in-plane symmetry for a 9-nm-thick, Te-capped film on InP (111). Reprinted from Figures 1 and 2 with permission from Winnerlein *et al.* ⁹⁷ Copyright (2017) by the American Physical Society.

to form antisite defects. As a result, the synthesis of the compound $(Bi_{1-x}Sb_x)_2Te_3$ offers a direct approach to balance out n- and p-type conduction. When $x\approx 0.95$, the carrier density was lowered 107 to 2×10^{12} cm $^{-2}$. This facilitated the observation of the QHE 144 , and ultimately the QAHE in Cr/V-doped BST $^{23-31,97,138}$. Figure 1 illustrates the structural properties of an optimally doped $V_{0.1}(Bi_{0.21}Sb_{0.79})_{1.9}Te_3$ film on Si $(111)^{97}$.

III. MATERIALS CHARACTERIZATION FOR QAHE RESISTANCE STANDARD

To realize BST devices as QAHE PRS, deterministic engineering of electronic and magnetic properties of the surface and the bulk is essential. A feedback loop between growth and QAHE performance has to be established, including material characterization at both macroscopic and nanoscopic scales as illustrated in Figure 2. Inhomogeneities of structural, electronic, and magnetic properties at the nanoscale have been previously shown to have adverse effects on the robustness of QAHE quantization. Consequently, there is a need to combine

bulk/macroscopic with surface-sensitive nanoscale characterization techniques, in order to distinguish bulk, surface, and edge properties, and to correlatively examine inhomogeneities that contribute to the high bulk conductivity.

A. Structural characterization

Structural properties of QAHE materials are commonly characterized in situ using RHEED147,148 [inset to Figure 1(a)], as well as ex situ techniques such as x-ray photoelectron spectroscopy (XPS)^{75,149,150}, x-ray diffraction and reflectometry (XRD, XRR)^{151–154} [Figure 1(a,b,d)], STM¹⁵⁵, and AFM¹⁴⁵,156 [Figure 1(c)]. Combined with other ex situ techniques, such as TEM with energy-dispersive X-ray spectroscopy (EDS)¹⁴⁸, Rutherford backscattering spectroscopy (RBS) and particle-induced X-ray emission (PIXE)¹⁵⁷, as well as synchrotron-based extended X-ray absorption fine structure (EXAFS)^{158,159}, the stoichiometry, dopant states and concentration in TIs can be determined. Basic principles and instruments for these techniques have been comprehensively covered in a previous review¹⁴⁵, which demonstrated that structural properties can be identified from macroscopic down to atomic level.

B. Electrical, electronic, and magnetic characterization

Electrical and magnetic properties are typically only characterized ex situ, which makes high lateral precision and especially tunability of the probing depth more demanding. Alternatively, development of in situ, MBE-compatible electromagnetic characterization techniques would be advantageous, but remains a challenge. Given the challenges of reducing impurity concentrations and their effect on the electron potential landscape, it is important to measure the electronic band structure of TI thin films to determine the Fermi level and validate the existence of topological surface states. Electronic band structures of TI thin films are often measured by ARPES, which maps the energy- and angle-resolved distribution of valence band electrons emitted upon ionization via high-energy photon irradiation, enabling the band structure to be mapped along different crystallographic directions. As ARPES often uses incident light from a discrete gas resonance in the vacuum ultraviolet range 136,160, the probing depth is limited to the order of 1 nm. By tuning the incident photon energy utilizing synchrotron radiation or rapidly developing high-photonenergy laser sources, photon-energy-dependent measurements can be realized to extend the range of the probing depth to tens of nanometers, providing a means for distinguishing the surface and the bulk 16,161-163. However, the spatial resolution is limited to \sim 50 μ m in conventional ARPES, given by the typical incident beam size, and to hundreds of nanometers for nano-ARPES limited by the focus provided by a Fresnel zone plate ¹⁶⁴, averaging over any nanoscale inhomogeneity.

At the macroscopic scale, low-precision magnetotransport can serve as an easily accessible pre-characterization technique to observe QAHE quantization and filter out devices with inferior performance. The selected devices can be further characterized in high-precision magnetotransport measurement systems operating at mK ranges currently required for metrology-grade QAHE quantization. Magnetotransport measurements can also provide spatially averaged values for inhomogeneities in electronic properties, such as characteristic quantum coherence lengths and energy scale of disorder potential due to charge puddles 104,165,166. While they can provide some insight into the effect of localized impurities, they are not surface-sensitive and cannot deliver spatially resolved analysis. Alongside magnetotransport, THz spectroscopy has emerged as a powerful non-contact tool for electrical characterization of TI thin films. The carrier scattering rates of TIs tend to fall within the THz frequency range, rendering THz radiation a low-energy probe capable of extracting carrier concentration, mobility, and lifetimes 167-172. However, farfield THz spectroscopy is diffraction-limited and not surfacesensitive, therefore does not directly probe the TI surface and only infers spatially averaged properties aided via modeling.

Bulk magnetic properties of QAHE materials are commonly characterized using SQUID, vibrating-sample magnetometry, and magneto-optic Kerr effect^{66,173}. To be able to characterize local and depth-resolved magnetic properties, more advanced techniques such as XMCD and polarized neutron reflectometry are required. The recent review article¹⁴⁵ provides a comprehensive overview of characterization techniques for magnetic properties of QAHE materials.

C. Towards the nanoscale: scanning probe techniques

Given that none of the techniques discussed above offers a tunable probing depth combined with nanoscale lateral resolution, we emphasize the importance of functional scanning probe microscopy (SPM), which allows local materials characterization at the nanoscale and can independently resolve edge, surface/subsurface, and bulk properties. Understanding nanoscale inhomogeneities of electronic and magnetic properties, including variations in charge carrier density, band bending effects, and the intricacies of magnetic structure, present significant challenges for QAHE metrology, making it a subject of considerable interest for the broader scientific community. There exists a multitude of complementary (opto-)electronic and magnetic SPM techniques, such as scattering-type SNOM^{174–176}, scanning SQUID^{177,178}, scanning microwave microscopy (SMM)¹⁷⁹, MFM, and Kelvin probe force microscopy (KPFM)¹⁸⁰. These methods intrinsically offer nanoscale spatial resolution typically below 50 nm, making them excellent choices for direct imaging of edge states and for nanoscale assessment of inhomogeneities in magnetically doped BST thin films and devices.

As an example, s-SNOM can perform optoelectronic characterization over a wide spectral range (visible-THz) beyond the diffraction limit^{181–184} and its probing depth can be controlled via the nonlinear tip-sample interaction^{174,185–187}. In conjunction with suitable modeling methods^{181,188–192}, s-SNOM can in principle distinguish electronic states and conductivity with nanoscale (<20 nm) resolution both lat-

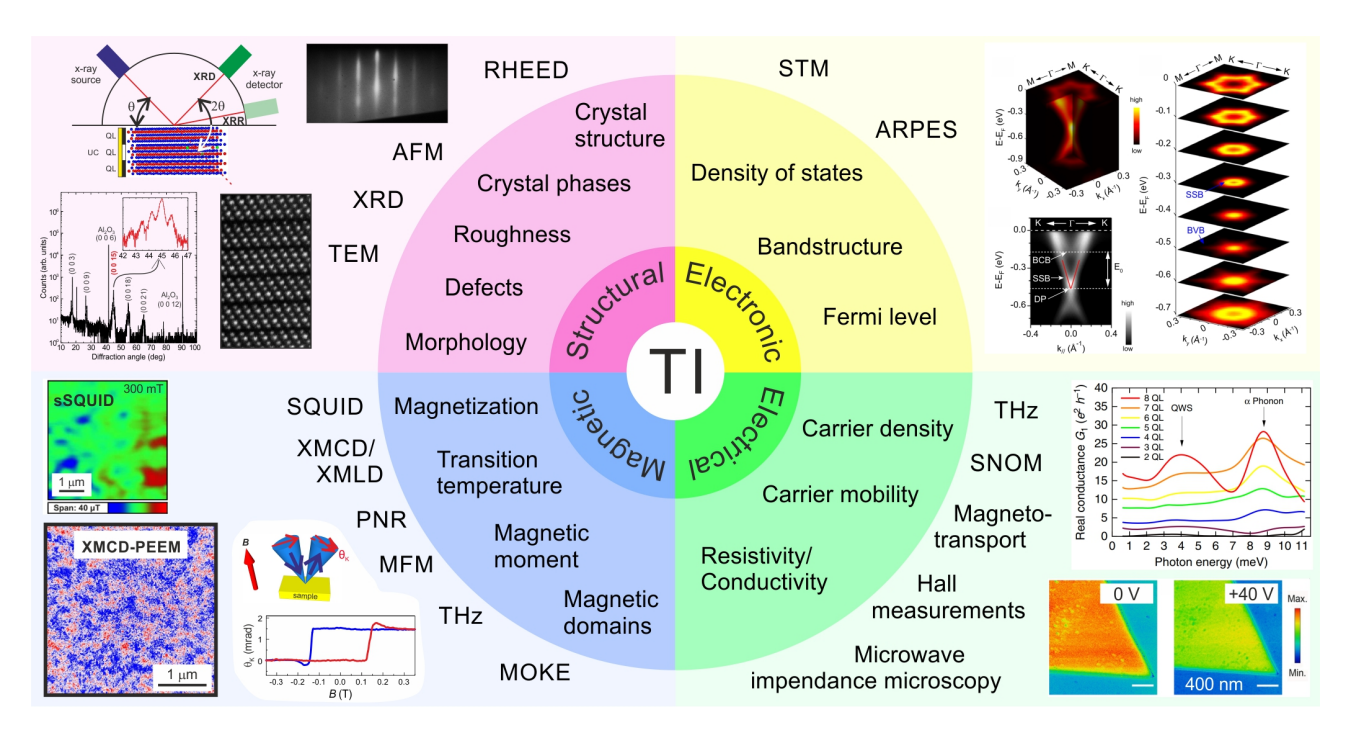


FIG. 2. Main classes of characterization techniques for QAHE materials, categorized into structural, electronic, electrical, and magnetic properties. Structural analysis relies on XRD, atomic force microscopy (AFM), transmission electron microscopy (TEM), and RHEED, each providing insights into crystal structures, phases, defects, and surface morphology. Electronic properties are explored using scanning tunneling microscopy (STM) and angle-resolved photoemission spectroscopy (ARPES), which examine the band structure, density of states, and the position of the Fermi level. Magnetic properties can be measured using techniques such as superconducting quantum interference device (SQUID) microscopy, X-ray magnetic circular dichroism photoemission electron microscopy (XMCD-PEEM), and magnetic force microscopy (MFM). Lastly, electrical properties can be assessed via scanning near-field optical microscopy (SNOM) and Hall measurements, providing carrier densities and mobilities. Together, these methods provide insight into the complex properties of TIs, essential for advancing their applications in technology. Top (left and right) and bottom left insets are reprinted from Liu *et al.* ¹⁴⁵ Bottom right insets are reprinted (adapted) with permission from Yuan *et al.* ¹⁴⁶ Copyright 2017 American Chemical Society.

erally and at different depths, hence useful for determining the effects of film thickness on hybridization of electronic states ^{174,193–195} and probing heterostructure interfaces and sub-surface dynamics. State-of-the-art s-SNOM can now operate at cryogenic temperatures below 10 K. Rapid instrumentational and metrological development ^{184,196,197} provides a realistic prospect of operation at even lower temperatures and incorporation of high magnetic fields, yet there is further need for good practices of s-SNOM modeling, quantitative and traceable determination of key transport and electromagnetic parameters towards more robust materials metrology ^{198–200}.

IV. QAHE METROLOGY

The realization of a quantum Hall resistance standard (QHRS) based on conventional materials requires high magnetic fields generated by superconducting solenoids. This limits the operation practicality and makes it technically challenging to integrate with the Josephson voltage standards (JVS) in a single cryogenic system^{201,202}. QAHE in magnetically doped BST has demonstrated Hall resistance quantization without a permanent external magnetic field^{23,24,27,29,30,32–36,202}. Early transport measurements aim-

ing at quantitative confirmation of Hall resistance quantization in the QAHE regime were performed on devices in Hall bar geometry [Figure 3(a,b)] using conventional equipment like calibrated resistors, voltage and current sources and detectors 27,29 . Since 2018, precision Hall resistance measurements at considerably higher accuracy levels were published, demonstrating Hall resistance quantization at the 10^{-6} level of relative uncertainty and better $^{7,32-36,202}$.

A. Cryogenic current comparators for resistance metrology

The majority of these studies used metrology-grade high-precision resistance bridges based on the concept of the cryogenic current comparator (CCC) and included evaluations of the measurement uncertainties. CCC-based bridges and quantum-referenced standard resistors are well-established in resistance metrology and key to resistance measurements at state-of-the-art accuracy levels at ten parts-per-billion and below^{203–206}. As the goal is to measure a resistance ratio by comparing an unknown resistor with a resistance reference, the bridge techniques designed to measure ratios are inherently superior to potentiometric methods. A simplified measurement scheme with a CCC-based technique is shown in

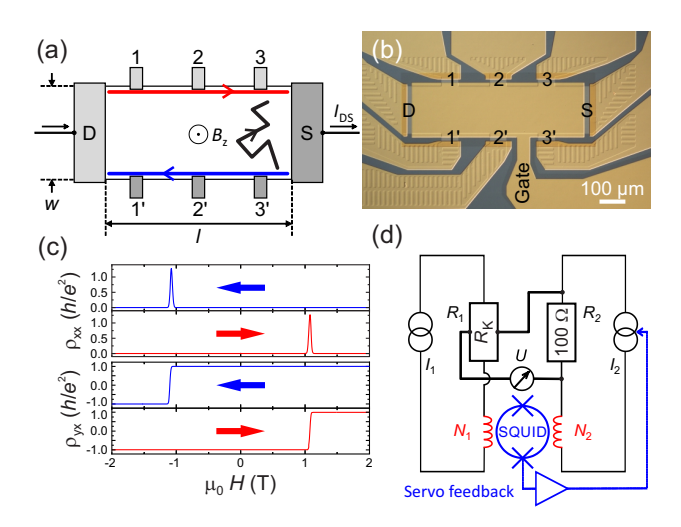


FIG. 3. (a) Schematics of a QHRS device in Hall bar geometry (width w and length l), with source (S), drain (D) and three pairs of Hall-voltage contacts (1-1' to 3-3'). The arrow represents the current flow for I_{DS} . (b) Nomarski microscope image of a $V_{0.1}(Bi_{0.2}Sb_{0.8})_{1.9}Te_3$ QAHE device³⁶. The gate electrode is used to tune the chemical potential in the TI film. (c) Hall resistivity ρ_{xy} and longitudinal resistivity ρ_{xx} versus external magnetic field as measured for the V-doped BST Hall bar device. As typical fingerprint of the QAHE, the Hall resistivity is quantized in terms of R_K for magnetic fields where the longitudinal resistivity vanishes (including at B=0). (d) Simplified schematic of a CCC resistance bridge used to measure the Hall resistance of a QAHE device.

Figure 3(d). The CCC fixes the ratio of the currents I_1 and I_2 , flowing through a QAHE device $R_1 = R_K$ and a calibrated reference resistor $R_2 = 100 \Omega$. The SQUID detects the magnetic flux proportional to the difference $N_1 \cdot I_1 - N_2 \cdot I_2$. The current I_2 is adjusted by a feedback loop controlled by the SQUID to null the difference, such that $I_1/I_2 = N_2/N_1$. The R_1/R_2 ratio is calculated from the numbers-of-turns ratio N_1/N_2 , from the bridge voltage difference U and from the voltage drop $I_2 \cdot R_2$ across the reference resistor. Further details on advanced design and performance of state-of-the-art CCC bridges are given elsewhere^{207–210}. Recent precision measurements on QAHE devices made from magnetically doped BST films were performed using bridges based on commercially available 32,33,35,202 or custom-made CCCs 7,36,211. For Hall resistance measurements targeting highest accuracy and precision, the restriction to low bias currents (≤100 nA) reflects in low fluxes generated by the windings of the CCC and coupling into the SQUID, which can limit the performance. Therefore, for measurements at very low currents the use of the highest possible numbers of turns N_1 and N_2 suitable for realizing $N_1/N_2 \approx R_2/R_1$ is favorable, resulting in minimizing the contribution of the SQUID to the uncertainty budget³⁶.

B. Practical aspects: QHRS guidelines and methods

General rules and best practices for the metrological application of the QHE in resistance metrology are laid out in technical guidelines²⁰⁵ for reliable dc measurements of the quantized Hall resistance. These guidelines describe the main tests and precautions necessary for both reproducible and accurate results in the use of the QHE to establish a reference standard of dc resistance with a relative uncertainty of a few parts in 10⁹. Although they are more specific for QHRS, the general methods and rules defined are also applicable to the QAHE resistance standard. QHRS devices are preferably shaped in a "Hall bar" geometry [Figure 3(a,b)]. In addition to the source and drain contacts for the bias current, they should be fitted with at least two pairs of contacts for measuring the Hall voltage, all of which providing galvanic connections to the conducting path of the device. For gated devices, an additional contact for applying a voltage to an electrostatic gate electrode is necessary, which should not have galvanic connection to the electron system.

Moreover, to have a reliable device, it is important that the Hall bar be large, such that the separation between opposite edges of the bar is much larger than the width of the edge state region. In this macroscopic limit, the main breakdown mechanism is scattering of electrons between conducting edge channels on different sides of the Hall bar, and therefore the critical current typically scales linearly with the width of the Hall bar, as observed in conventional QHRS devices²¹². For the QAHE in the macroscopic limit, it is believed that the breakdown mechanism is caused by electric-field-driven percolation of charge puddles in the surface states of the TI films. Similar to conventional QHRS, a linear relationship between the critical current and the Hall bar width was observed^{89–91}. Thus, the width of the Hall bar should be sufficiently large $(100-800 \mu m)$, with the maximum size usually limited by the homogeneity of the TI films^{7,32–36,202}. The source and drain current contacts should extend over the whole width of the device to maximize the critical current. Narrow voltage contacts should be avoided, as this can lead to non-equilibrium populations of the electronic edge states and partial depletion of the 2DES in the narrow channels, which will cause deviations of the Hall voltage from the nominal quantized value R_K in the QAHE regime. The distances between the voltage contact pairs should be sufficiently large, i.e., in the order of the width of the device 205 .

Another important aspect is quality of the device fabrication. While initially the experimental reports of QAHE often relied on mechanical scratching to define Hall bar-shaped structures²⁴, recent metrology-grade experiments rely solely on lithographically patterned devices^{7,32–36}. A top gate is employed to electrostatically tune the Fermi level and minimize the parasitic bulk conductivity, enabling pure edge state transport (a back gate should in principle work equally well for this purpose, but that has not yet been tested to metrological precision). While details of gate geometry are not expected to be relevant for DC resistance metrology, at AC frequencies, circuit capacitance considerations will obviously have to include the exact gating geometry.

The key feature of QHEs (including QAHE) is the occurrence of Hall (transverse) resistance quantization together with vanishing longitudinal resistance, when entering the regime of dissipationless transport along the edge channels

Probing Depth & Resolution

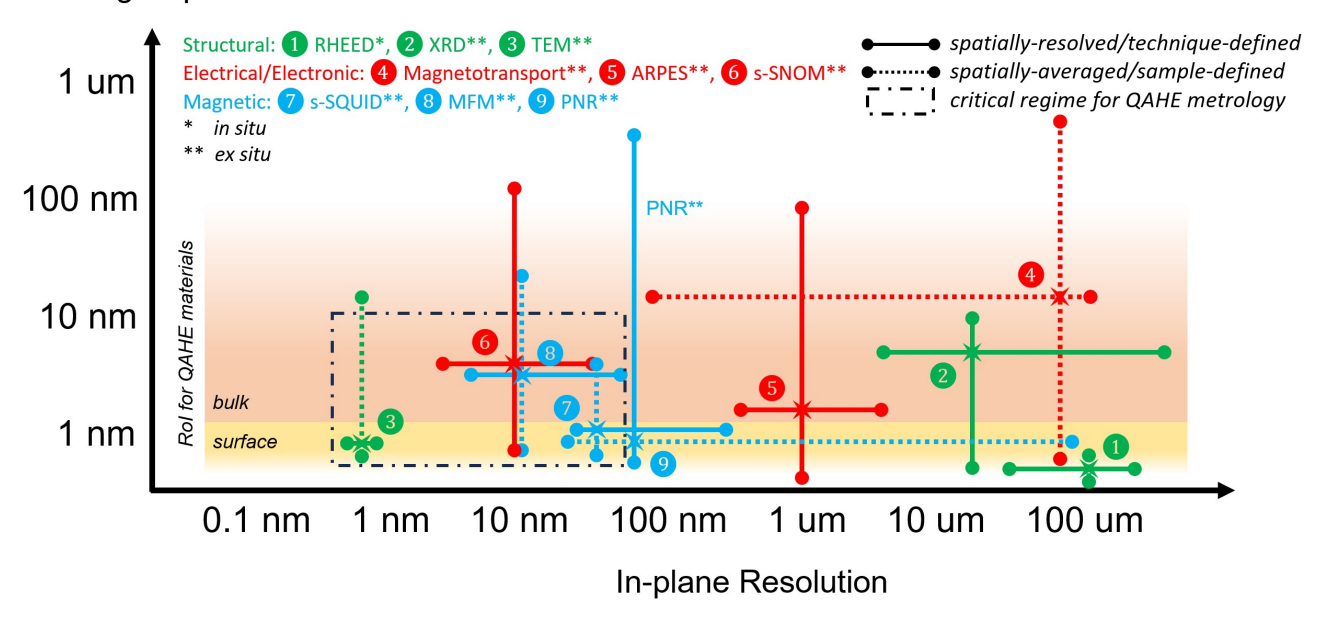


FIG. 4. Comparative analysis of several essential characterization methods for QAHE materials with regards to probing depth and spatial resolution. Horizontal and vertical lines represent the tunability of in-plane and depth resolution, respectively; their intersections represent typical spatial resolution. The dash-dotted box highlights the critical regime required for the development of robust QAHE PRS.

[Figure 3(c)]. Realizing this transport regime requires adjusting the chemical potential so that bulk conductivity is suppressed to the minimum. The respective tuning of QHRS devices is preferably carried out by minimizing the longitudinal resistance (or voltage) measured along the device [on two opposite pairs of voltage contacts, 1-3 or 1'-3' in Figure 3(a,b)]. More accurate results are obtained by carrying out measurements of transverse voltages on several contact pairs including "orthogonal" and "diagonal" contacts, and then by calculating the longitudinal voltage by using Kirchhoff's voltage law²⁰⁵.

Non-ideal voltage contacts to the electron system can severely affect precision measurements and are critical for the device performance in metrology²⁰⁵. Besides causing excessive current or voltage noise, poor voltage contacts can generate offset voltages which introduce systematic errors in measurements of the Hall resistance due to noise rectification processes. As poor contacts are typically indicated by elevated contact resistance (and, in the worst case, by non-linear current-voltage characteristics), contact resistances should be determined prior to precision measurements of the QAHE. A practical method to perform contact resistance measurements uses a three-terminal measurement technique²⁰⁵. For conventional QHRS devices, typical contact resistances of highquality contacts are of the order 10 Ω or below; however, higher contact resistances up to 100Ω are acceptable²⁰⁵. For magnetically doped BST QAHE devices, contact resistances as low as several ohm were reported^{7,33,36,211}. For achieving low contact resistances, choosing a split-finger design of the contacts implementing a miniature on-chip multiple terminal connection can be useful²¹³, as demonstrated for graphenebased devices²¹⁴.

Besides the determination of contact resistances, the quan-

titative evaluation of the residual longitudinal resistivity ρ_{xx} is key to the conditions of Hall resistance quantization in all known types of QHE devices. Ideally, the value of the transverse resistivity ρ_{xy} on the resistance plateau is, within the limit of the resolution of the measurements, invariant over appreciable ranges of relevant experimental parameters like bias current or temperature. If bias current or temperature are increased beyond critical limits, the breakdown of the QHE with a deviation of ρ_{xy} from the quantized value occurs^{204,205}. Generally, this is indicated by a gradual increase of ρ_{xx} . The dependence of ρ_{xy} on ρ_{xx} typically depends on the device geometry, the operating conditions, the magnetic field direction, the position on the resistance plateau, and the bias current^{203–205}. In QHRS devices, it has often been observed that ρ_{xy} varies linearly with ρ_{xx} over several decades in ρ_{xx} , described by the relationship $\delta \rho_{xx} = s \cdot \rho_{xx}$, with $\delta \rho_{xy} = \rho_{xy}/R_K - 1$ being the deviation of the Hall resistivity ρ_{xy} relative to $R_K^{204,205,215-219}$. In case of thermal activation, this behavior stems from the temperature dependence of ho_{xx} and the geometrical mixing of the longitudinal voltage into the Hall voltage. In conventional OHRS devices, experimentally determined values of the proportionality factor s typically vary between -1 and -0.01. For QAHE devices made from magnetically doped BST films, values between about -0.1 and -0.01 were reported^{7,36}. In some cases, deviations from a linear $\rho_{xy}(\rho_{xx})$ relationship were observed^{33,211}. The dependence of ρ_{xy} on ρ_{xx} is of particular significance in quantum Hall resistance metrology. Analysis of $\delta \rho_{xy}(\rho_{xx})$ when extrapolated to $\rho_{xx} = 0$ (dissipationless transport)^{204,215,217,219–222} yields a proper measure for Hall resistance quantization under ideal conditions, allowing QAHE device performance evaluation for QHRS

applications^{7,33,36}.

V. METROLOGICAL OUTLOOK FOR QAHE

A. Materials optimization and metrological characterization

The necessity of introducing magnetic order in TI films has spurred extensive research aimed at identifying the optimal dopant – one that introduces magnetic order, while not being detrimental to the electronic properties. Both transition metal (TM) and rare earth doped TI films exhibit promising characteristics²²³. While ferromagnetic order has been reported in a number of TM-doped TIs, Cr and V possess the most robust long-range ferromagnetic order with the desired out-of-plane anisotropy and a typical T_C of 59 K (104 K) for Cr (V) concentrations of x = 0.29 (0.25) in Sb_{2-x}(V/Cr)_xTe₃³⁰. As the QAHE is limited to temperatures far below their ferromagnetic ordering temperatures, magnetic doping is still an open material challenge.

To address the challenge of the non-insulating bulk, Figure 4 compares several essential characterization methods required for QAHE materials. Their variations in probing depth, spatial resolution, and their alignment with the critical regime of interest for robust QAHE resistance standards are shown. Most current techniques do not offer a tunable probing depth on the nanometer regime - a central obstacle for OAHE materials optimization. While s-SNOM represents a prime example of a tomographic technique with nanoscale resolution and tunability in all three dimensions, its application is confined in electronic and optical characterization. Therefore, we emphasize the importance of integrating complementary, multifunctional, and multiscale techniques. Concurrently, there is a need for development of in-situ, local and depth-sensitive electronic and magnetic characterization methods, which can also reduce material degradation and contamination that can occur during ex situ material evaluations. To further develop and reliably employ these techniques, while ensuring high accuracy and precision, metrological improvements to most of the abovementioned techniques are needed, namely: establishing practical standards of measurements, modeling techniques, and reference materials; defining and assuring unbroken chains of traceability to practical realizations of the SI units; better understanding the sources of variability and inaccuracy, improving reproducibility and comparability. We emphasize that only with these rigorous metrological approaches, we can progress metrological materials characterization to enable real-world innovations of TIs with confidence.

$\label{eq:B.Vision} \textbf{B. Vision, strategies, and challenges for practical QAHE metrology}$

Main motivations for the development of a QHRS operatable at zero external magnetic field are, *i*) it is important for practical quantum electrical metrology, providing the attractive possibility to integrate a QHRS and a JVS in a single cryogenic apparatus, without hampering the operation of

the JVS by magnetic fields needed for the QHRS operation; ii) it is of an economical nature, i.e., to save the costs and technical efforts associated with the operation of high-field magnets, enabling wider dissemination of electrical units directly to end users and incorporation of precision metrology into routine calibrations in different economic sectors. The full practical and economic advantages of such integrated systems will be exploited using cryogen-free systems, such as a pulse-tube cryocooler with closed helium or helium-free circuits and small laboratory footprint. Commercial state-of-theart cryocoolers can achieve temperatures down to about 2 K in combination with magnets sufficient to magnetize the QAHE device prior to operation. Such compact system would realize a universal "quantum electrical metrology toolbox" and offer the possibility to perform resistance, voltage and current metrology based on the primary quantum electrical effects. This strategic target is at the heart of modern quantum electrical metrology, which aims to develop and provide userfriendly, economic quantum standard systems for an extended usership suitable for direct exploitation by industry. Presently, several metrological institutes worldwide are working toward this direction. The National Institute of Standards and Technology (USA) recently implemented a quantum current sensor setup that combines a QAHE device and a JVS in a single cryostat²⁰². With this, currents within the range 10-250 nA were measured with relative uncertainty 4-40 parts per million. However, the operation of QAHE device yet requires a dilution refrigerator, therefore, currently does not meet the desired requirements for practicality, affordability, or mobility. Furthermore, Rodenbach et al.²⁰² reported significant heating of the quantum anomalous Hall device due to microwave radiation leakage from the programmable Josephson voltage standard in their setup, demonstrating that complications can arise from integrating a QAHE device with a JVS in a single dilution refrigerator. Generally, such integration is challenging since dilution refrigerators with millikelvin base temperatures have cooling powers limited to a few hundreds of microwatts typically, which imposes technical constraints on the acceptable heat load introduced by the wiring or by radiation sources of the system. These limitations are less severe, for instance, for pulse-tube cryocooler systems which offer cooling powers of the order of a watt typically. However, due to the temperature limitations set by state-of-the-art QAHE devices, the integration with the JVS in a cryocooler is currently not possible.

Regarding one of the main metrological benchmarks – the quantization accuracy – state-of-the-art QAHE devices have recently demonstrated performance at the 10^{-9} level in measurements performed at the National Metrology Institute of Japan and at the Physikalisch-Technische Bundesanstalt (Germany)^{7,36}. This complies with the needs of metrological applications^{203–206} and holds promise for future further developments. Regarding the matter of increasing the applicable bias currents to the metrologically desired level beyond few μ A⁷, novel concepts based on advanced device layouts and operation schemes were proposed, and proof-of-principle experiments already showed promising results^{92,114}. Currently, these schemes are undergoing validation at accuracy levels

relevant for metrological applications.

Most pressing need for practical QAHE metrology and resistance standards, therefore, is the remaining task to overcome the limitations regarding temperatures requiring dilution refrigerator operation. The current consensus is that this will also require significant improvements in the field of materials science and technology to explore novel material systems beyond the family of magnetically doped BST. These routes toward QAHE realizations at temperatures of at least 1 K are consequently pursued as part of the current European Partnership on Metrology project "Quantum Anomalous Hall Effect Materials and Devices for Metrology"²²⁴.

ACKNOWLEDGMENTS

The authors would like to acknowledge the support via the project "Quantum Anomalous Hall Effect Materials and Devices for Metrology" (QuAHMET). The project (23FUN07 QuAHMET) has received funding from the European Partnership on Metrology, co-financed from the European Union's Horizon Europe Research and Innovation Programme and by the Participating States. N.J.H., J.L.B., and O.K. acknowledge the support of the UK government Department for Science, Innovation and Technology through the UK National Quantum Technologies Programme. J.L.B also acknowledges UKRI the financial support via her Future Leaders Fellowship (MR/T022140/1); EPSRC via the NAME program grant (EP/V001914/1) and EP/T01914X/1; and the Henry Royce Institute for their support. H.S. gratefully acknowledges the financial support by the European Commission under the H2020 FETPROACT Grant TOCHA (824140), by EMPIR 20FUN03 COMET (this project has received funding from the EMPIR program co-financed by the Participating States and from the European Union's Horizon 2020 research and innovation program), and by the Deutsche Forschungsgemeinschaft (EXC-2123 QuantumFrontiers, 390837967). K.M.F. and C.G. gratefully acknowledge the financial support of the Free State of Bavaria (the Institute for Topological Insulators), Deutsche Forschungsgemeinschaft (SFB 1170, 258499086), Würzburg-Dresden Cluster of Excellence on Complexity and Topology in Quantum Matter (EXC 2147, 39085490), and the European Commission under the H2020 FETPROACT Grant TOCHA (824140).

CONFLICT OF INTEREST

The authors have no conflicts to disclose.

DATA AVAILABILITY

The data that support the discussions of this article are available from the corresponding authors upon reasonable request.

AUTHORS CONTRIBUTIONS

N.J.H.: Conceptualization (equal); Data Curation (equal); Formal Analysis (equal); Funding Acquisition (equal); Investigation (equal); Methodology (equal); Resources (equal); Visualization (equal); Writing/Original Draft Preparation (equal); Writing/Review and Editing (equal); Project Administration (lead). J.L.B.: Conceptualization (equal); Data Curation (equal); Formal Analysis (equal); Funding Acquisition (equal); Investigation (equal); Methodology (equal); Resources (equal); Visualization (equal); Writing/Original Draft Preparation (equal); Writing/Review and Editing (equal). **K.M.F.**: Conceptualization (equal); Data Curation (equal); Formal Analysis (equal); Investigation (equal); Methodology (equal); Resources (equal); Visualization (equal); Writing/Original Draft Preparation (equal); Writing/Review and Editing (equal). C.G.: Conceptualization (equal); Data Curation (equal); Formal Analysis (equal); Funding Acquisition (equal); Investigation (equal); Methodology (equal); Resources (equal); Visualization (equal); Writing/Original Draft Preparation (equal); Writing/Review and Editing (equal). T.H.: Conceptualization (equal); Data Curation (equal); Formal Analysis (equal); Funding Acquisition (equal); Investigation (equal); Methodology (equal); Resources (equal); Visualization (equal); Writing/Original Draft Preparation (equal); Writing/Review and Editing (equal). O.K.: Conceptualization (equal); Data Curation (equal); Formal Analysis (equal); Funding Acquisition (equal); Investigation (equal); Methodology (equal); Resources (equal); Visualization (equal); Writing/Original Draft Preparation (equal); Writing/Review and Editing (equal). S.K.: Conceptualization (equal); Data Curation (equal); Formal Analysis (equal); Funding Acquisition (equal); Investigation (equal); Methodology (equal); Resources (equal); Visualization (equal); Writing/Original Draft Preparation (equal); Writing/Review and Editing (equal). H.S.: Conceptualization (equal); Data Curation (equal); Formal Analysis (equal); Funding Acquisition (equal); Investigation (equal); Methodology (equal); Resources (equal); Visualization (equal); Writing/Original Draft Preparation (equal); Writing/Review and Editing (equal).

¹E. H. Hall, "On a new action of the magnet on electric currents," Am. J. Math. **2**, 287 (1879).

²K. von Klitzing, G. Dorda, and M. Pepper, "New method for high-accuracy determination of the fine-structure constant based on quantized Hall resistance," Phys. Rev. Lett. 45, 494 (1980).

³M. Stock, R. Davis, E. de Mirandés, and M. J. T. Milton, "The revision of the SI – the result of three decades of progress in metrology," Metrologia **56**, 022001 (2019).

⁴Y. Zhang, Y.-W. Tan, H. L. Stormer, and P. Kim, "Experimental observation of the quantum Hall effect and Berry's phase in graphene," Nature 438, 201 (2005).

⁵A. Tzalenchuk, S. Lara-Avila, A. Kalaboukhov, S. Paolillo, M. Syväjärvi, R. Yakimova, O. Kazakova, T. J. B. M. Janssen, V. Fal'ko, and S. Kubatkin, "Towards a quantum resistance standard based on epitaxial graphene," Nat. Nanotechnol. 5, 186 (2010).

⁶A. Chatterjee, M. Kruskopf, M. Götz, Y. Yin, E. Pesel, P. Gournay, B. Rolland, J. Kučera, S. Bauer, K. Pierz, B. Schumacher, and H. Scherer, "Performance and stability assessment of graphene-based quantum Hall devices for resistance metrology," IEEE Trans. Instrum. Meas. 72, 1 (2023).

⁷Y. Okazaki, T. Oe, M. Kawamura, R. Yoshimi, S. Nakamura, S. Takada, M. Mogi, K. S. Takahashi, A. Tsukazaki, M. Kawasaki, Y. Tokura, and

- N.-H. Kaneko, "Quantum anomalous Hall effect with a permanent magnet defines a quantum resistance standard," Nat. Phys. 18, 25 (2022).
- ⁸M. Onoda and N. Nagaona, "Quantized anomalous Hall effect in twodimensional ferromagnets: quantum Hall effect in metals," Phys. Rev. Lett. 90, 206601 (2003).
- ⁹C. L. Kane and E. J. Mele, "Z2 topological order and the quantum spin Hall effect," Phys. Rev. Lett. **95**, 146802 (2005).
- ¹⁰C. L. Kane and E. J. Mele, "Quantum spin Hall effect in graphene," Phys. Rev. Lett. 95, 226801 (2005).
- ¹¹B. A. Bernevig, T. L. Hughes, and S.-C. Zhang, "Quantum spin Hall effect and topological phase transition in HgTe quantum wells," Science 314, 1757 (2006).
- ¹²J. E. Moore and L. Balents, "Topological invariants of time-reversal-invariant band structures," Phys. Rev. B 75, 121306 (2007).
- ¹³L. Fu, C. L. Kane, and E. J. Mele, "Topological insulators in three dimensions," Phys. Rev. Lett. **98**, 106803 (2007).
- ¹⁴L. Fu and C. L. Kane, "Topological insulators with inversion symmetry," Phys. Rev. B 76, 045302 (2007).
- ¹⁵M. König, S. Wiedmann, C. Brüne, A. Roth, H. Buhmann, L. W. Molenkamp, X.-L. Qi, and S.-C. Zhang, "Quantum spin Hall insulator state in HgTe quantum wells," Science 318, 766 (2007).
- ¹⁶D. Hsieh, D. Qian, L. Wray, Y. Xia, Y. S. Hor, R. J. Cava, and M. Z. Hasan, "A topological Dirac insulator in a quantum spin Hall phase," Nature 452, 970 (2008).
- ¹⁷M. Z. Hasan and C. L. Kane, "Colloquium: topological insulators," Rev. Mod. Phys. 82, 3045 (2010).
- ¹⁸C.-X. Liu, X.-L. Qi, X. Dai, Z. Fang, and S.-C. Zhang, "Quantum anomalous Hall effect in Hg_{1-y}Mn_yTe quantum wells," Phys. Rev. Lett. 101, 146802 (2008).
- ¹⁹M. König, H. Buhmann, L. W. Molenkamp, T. Hughes, C.-X. Liu, X.-L. Qi, and S.-C. Zhang, "The quantum spin Hall effect: theory and experiment," J. Phys. Soc. Jpn. 77, 031007 (2008).
- ²⁰J. K. Furdyna, "Diluted magnetic semiconductors," J. Appl. Phys. 64, R29 (1988).
- ²¹S. Shamim, W. Beugeling, J. Böttcher, P. Shekhar, A. Budewitz, P. Leubner, L. Lunczer, E. M. Hankiewicz, H. Buhmann, and L. W. Molenkamp, "Emergent quantum Hall effects below 50 mT in a two-dimensional topological insulator," Sci. Adv. 6, eaba4625 (2020).
- ²²H. Zhang, C.-X. Liu, X.-L. Qi, X. Dai, Z. Fang, and S.-C. Zhang, "Topological insulators in Bi₂Se₃, Bi₂Te₃ and Sb₂Te₃ with a single Dirac cone on the surface," Nat. Phys. 5, 438 (2009).
- ²³R. Yu, W. Zhang, H.-J. Zhang, S.-C. Zhang, X. Dai, and Z. Fang, "Quantized anomalous Hall effect in magnetic topological insulators," Science 329, 61 (2010).
- ²⁴C.-Z. Chang, J. Zhang, X. Feng, J. Shen, Z. Zhang, M. Guo, K. Li, Y. Ou, P. Wei, L.-L. Wang, Z.-Q. Ji, Y. Feng, S. Ji, X. Chen, J. Jia, X. Dai, Z. Fang, S.-C. Zhang, K. He, Y. Wang, L. Lu, X.-C. Ma, and Q.-K. Xue, "Experimental observation of the quantum anomalous Hall effect in a magnetic topological insulator," Science 340, 167 (2013).
- ²⁵ J. G. Checkelsky, R. Yoshimi, A. Tsukazaki, K. S. Takahashi, Y. Kozuka, J. Falson, M. Kawasaki, and Y. Tokura, "Trajectory of the anomalous Hall effect towards the quantized state in a ferromagnetic topological insulator," Nat. Phys. 10, 731 (2014).
- ²⁶X. Kou, S.-T. Guo, Y. Fan, L. Pan, M. Lang, Y. Jiang, Q. Shao, T. Nie, K. Murata, J. Tang, Y. Wang, L. He, T.-K. Lee, W.-L. Lee, and K. L. Wang, "Scale-invariant quantum anomalous Hall effect in magnetic topological insulators beyond the two-dimensional limit," Phys. Rev. Lett. 113, 137201 (2014)
- ²⁷ A. J. Bestwick, E. J. Fox, X. Kou, L. Pan, K. L. Wang, and D. Goldhaber-Gordon, "Precise quantization of the anomalous Hall effect near zero magnetic field," Phys. Rev. Lett. 114, 187201 (2015).
- ²⁸A. Kandala, A. Richardella, S. Kempinger, C.-X. Liu, and N. Samarth, "Giant anisotropic magnetoresistance in a quantum anomalous Hall insulator," Nat. Commun. 6, 7434 (2015).
- ²⁹C.-Z. Chang, W. Zhao, D. Y. Kim, P. Wei, J. K. Jain, C. Liu, M. H. W. Chan, and J. S. Moodera, "Zero-field dissipationless chiral edge transport and the nature of dissipation in the quantum anomalous Hall state," Phys. Rev. Lett. 115, 057206 (2015).
- ³⁰C.-Z. Chang, W. Zhao, D. Y. Kim, H. Zhang, B. A. Assaf, D. Heiman, S.-C. Zhang, C. Liu, M. H. W. Chan, and J. S. Moodera, "High-precision

- realization of robust quantum anomalous Hall state in a hard ferromagnetic topological insulator," Nat. Mater. 14, 473 (2015).
- ³¹S. Grauer, S. Schreyeck, M. Winnerlein, K. Brunner, C. Gould, and L. W. Molenkamp, "Coincidence of superparamagnetism and perfect quantization in the quantum anomalous Hall state," Phys. Rev. B 92, 201304 (2015).
- ³²M. Gótz, K. M. Fijalkowski, E. Pesel, M. Hartl, S. Schreyeck, M. Winnerlein, S. Grauer, H. Scherer, K. Brunner, C. Gould, F. J. Ahlers, and L. W. Molenkamp, "Precision measurement of the quantized anomalous Hall resistance at zero magnetic field," Appl. Phys. Lett. 112, 072102 (2018).
- ³³E. J. Fox, I. T. Rosen, Y. Yang, G. R. Jones, R. E. Elmquist, X. Kou, L. Pan, K. L. Wang, and D. Goldhaber-Gordon, "Part-per-million quantization and current-induced breakdown of the quantum anomalous Hall effect," Phys. Rev. B 98, 075145 (2018).
- ³⁴ Y. Okazaki, T. Oe, M. Kawamura, R. Yoshimi, S. Nakamura, S. Takada, M. Mogi, K. S. Takahashi, A. Tsukazaki, M. Kawasaki, Y. Tokura, and N.-H. Kaneko, "Precise resistance measurement of quantum anomalous Hall effect in magnetic heterostructure film of topological insulator," Appl. Phys. Lett. 116, 143101 (2020).
- ³⁵L. K. Rodenbach, A. R. Panna, S. U. Payagala, I. T. Rosen, M. P. Andersen, P. Zhang, L. Tai, K. L. Wang, D. G. Jarrett, R. E. Elmquist, D. B. Newell, D. Goldhaber-Gordon, and A. F. Rigosi, "Metrological assessment of quantum anomalous Hall properties," Phys. Rev. Appl. 18, 034008 (2022).
- ³⁶D. K. Patel, K. M. Fijalkowski, M. Kruskopf, N. Liu, M. Götz, E. Pesel, M. Jaime, M. Klement, S. Schreyeck, K. Brunner, C. Gould, L. W. Molenkamp, and H. Scherer, "Zero external magnetic field quantum standard of resistance at the 10⁻⁹ level," Nat. Electron. 7, 1111 (2024).
- ³⁷C.-Z. Chang, C.-X. Liu, and A. H. MacDonald, "Colloquium: Quantum anomalous Hall effect," Rev. Mod. Phys. 95, 011002 (2023).
- ³⁸J. Wang, B. Lian, and S.-C. Zhang, "Universal scaling of the quantum anomalous Hall plateau transition," Phys. Rev. B 89, 085106 (2014).
- ³⁹ X. Kou, L. Pan, J. Wang, Y. Fan, E. S. Choi, W.-L. Lee, T. Nie, K. Murata, Q. Shao, S.-C. Zhang, and K. L. Wang, "Metal-to-insulator switching in quantum anomalous Hall states," Nat. Commun. 6, 8474 (2015).
- ⁴⁰M. Kawamura, M. Mogi, R. Yoshimi, A. Tsukazaki, Y. Kozuka, K. S. Takahashi, M. Kawasaki, and Y. Tokura, "Topological quantum phase transition in magnetic topological insulator upon magnetization rotation," Phys. Rev. B 98, 140404 (2018).
- ⁴¹A. M. M. Pruisken, "Dilute instanton gas as the precursor to the integral quantum Hall effect," Phys. Rev. B 32, 2636 (1985).
- ⁴²A. M. M. Pruisken, "Universal singularities in the integral quantum Hall effect," Phys. Rev. Lett. 61, 1297 (1988).
- ⁴³S. Kivelson, D.-H. Lee, and S.-C. Zhang, "Global phase diagram in the quantum Hall effect," Phys. Rev. B 46, 2223 (1992).
- ⁴⁴A. M. Dykhne and I. M. Ruzin, "Theory of the fractional quantum Hall effect: the two-phase model," Phys. Rev. B 50, 2369 (1994).
- ⁴⁵I. Ruzin and S. Feng, "Universal relation between longitudinal and transverse conductivities in quantum Hall effect," Phys. Rev. Lett. **74**, 154 (1995).
- ⁴⁶M. Hilke, D. Shahar, S. H. Song, D. C. Tsui, Y. H. Xie, and M. Shayegan, "Semicircle: an exact relation in the integer and fractional quantum Hall effect," Europhys. Lett. 46, 775 (1999).
- ⁴⁷K. M. Fijalkowski, N. Liu, M. Hartl, M. Winnerlein, P. Mandal, A. Coschizza, A. Fothergill, S. Grauer, S. Schreyeck, K. Brunner, M. Greiter, R. Thomale, C. Gould, and L. W. Molenkamp, "Any axion insulator must be a bulk three-dimensional topological insulator," Phys. Rev. B 103, 235111 (2021).
- ⁴⁸F. Wilczek, "Two applications of axion electrodynamics," Phys. Rev. Lett. 58, 1799 (1987).
- ⁴⁹X.-L. Qi, T. L. Hughes, and S.-C. Zhang, "Topological field theory of time-reversal invariant insulators," Phys. Rev. B 78, 195424 (2008).
- ⁵⁰A. M. Essin, J. E. Moore, and D. Vanderbilt, "Magnetoelectric polarizability and axion electrodynamics in crystalline insulators," Phys. Rev. Lett. 102, 146805 (2009).
- ⁵¹X.-L. Qi and S.-C. Zhang, "Topological insulators and superconductors," Rev. Mod. Phys. 83, 1057 (2011).
- ⁵²K. Nomura and N. Nagaosa, "Surface-quantized anomalous Hall current and the magnetoelectric effect in magnetically disordered topological insulators," Phys. Rev. Lett. **106**, 166802 (2011).

- ⁵³J. Wang, B. Lian, X.-L. Qi, and S.-C. Zhang, "Quantized topological magnetoelectric effect of the zero-plateau quantum anomalous Hall state," Phys. Rev. B **92**, 081107 (2015).
- ⁵⁴T. Morimoto, A. Furusaki, and N. Nagaosa, "Topological magnetoelectric effects in thin films of topological insulators," Phys. Rev. B **92**, 085113 (2015).
- ⁵⁵W.-K. Tse and A. H. MacDonald, "Giant magneto-optical Kerr effect and universal Faraday effect in thin-film topological insulators," Phys. Rev. Lett. 105, 057401 (2010).
- ⁵⁶J. Maciejko, X.-L. Qi, H. D. Drew, and S.-C. Zhang, "Topological quantization in units of the fine structure constant," Phys. Rev. Lett. **105**, 166803 (2010).
- ⁵⁷M. Mogi, M. Kawamura, R. Yoshimi, A. Tsukazaki, Y. Kozuka, N. Shi-rakawa, K. S. Takahashi, M. Kawasaki, and Y. Tokura, "A magnetic heterostructure of topological insulators as a candidate for an axion insulator," Nat. Mater. 16, 516 (2017).
- ⁵⁸S. Grauer, K. M. Fijalkowski, S. Schreyeck, M. Winnerlein, K. Brunner, R. Thomale, C. Gould, and L. W. Molenkamp, "Scaling of the quantum anomalous Hall effect as an indicator of axion electrodynamics," Phys. Rev. Lett. 118, 246801 (2017).
- ⁵⁹M. Mogi, M. Kawamura, A. Tsukazaki, R. Yoshimi, K. S. Takahashi, M. Kawasaki, and Y. Tokura, "Tailoring tricolor structure of magnetic topological insulator for robust axion insulator," Sci. Adv. 3, eaao1669 (2018).
- ⁶⁰D. Xiao, J. Jiang, J.-H. Shin, W. Wang, F. Wang, Y.-F. Zhao, C. Liu, W. Wu, M. H. W. Chan, N. Samarth, and C.-Z. Chang, "Realization of the axion insulator state in quantum anomalous Hall sandwich heterostructures," Phys. Rev. Lett. 120, 056801 (2018).
- ⁶¹X. Wu, D. Xiao, C.-Z. Chen, J. Sun, L. Zhang, M. H. W. Chan, N. Samarth, X. C. Xie, X. Lin, and C.-Z. Chang, "Scaling behavior of the quantum phase transition from a quantum-anomalous-Hall insulator to an axion insulator," Nat. Commun. 11, 4532 (2020).
- ⁶²M. Mogi, Y. Okamura, M. Kawamura, R. Yoshimi, K. Yasuda, A. Tsukazaki, K. S. Takahashi, T. Morimoto, N. Nagaosa, M. Kawasaki, Y. Takahashi, and Y. Tokura, "Experimental signature of the parity anomaly in a semi-magnetic topological insulator," Nat. Phys. 18, 390 (2022).
- ⁶³D. Zhuo, Z.-J. Yan, Z.-T. Sun, L.-J. Zhou, Y.-F. Zhao, R. Zhang, R. Mei, H. Yi, K. Wang, M. H. W. Chan, C.-X. Liu, K. T. Law, and C.-Z. Chang, "Axion insulator state in hundred-nanometer-thick magnetic topological insulator sandwich heterostructures," Nat. Commun. 14, 7596 (2023).
- ⁶⁴L.-X. Wang, W. Beugeling, F. Schmitt, L. Lunczer, J.-B. Mayer, H. Buhmann, E. M. Hankiewicz, and L. W. Molenkamp, "Spectral asymmetry induces a re-entrant quantum Hall effect in a topological insulator," Adv. Sci. 11, 2307447 (2024).
- ⁶⁵L. Wu, M. Salehi, N. Koirala, J. Moon, S. Oh, and N. P. Armitage, "Quantized Faraday and Kerr rotation and axion electrodynamics of a 3D topological insulator," Science 354, 6316 (2016).
- ⁶⁶K. N. Okada, Y. Takahashi, M. Mogi, R. Yoshimi, A. Tsukazaki, K. S. Takahashi, N. Ogawa, M. Kawasaki, and Y. Tokura, "Terahertz spectroscopy on Faraday and Kerr rotations in a quantum anomalous Hall state," Nat. Commun. 7, 12245 (2016).
- ⁶⁷ V. Dziom, A. Shuvaev, A. Pimenov, G. V. Astakhov, C. Ames, K. Bendias, J. Böttcher, G. Tkachov, E. M. Hankiewicz, C. Brüne, H. Buhmann, and L. W. Molenkamp, "Observation of the universal magnetoelectric effect in a 3D topological insulator," Nat. Commun. 8, 15197 (2017).
- ⁶⁸C. Berger, F. Bayer, L. W. Molenkamp, and T. Kiessling, "Diminishing topological Faraday effect in thin layer samples," Phys. Rev. Res. 6, 013068 (2024).
- ⁶⁹ X. Kou, M. Lang, Y. Fan, Y. Jiang, T. Nie, J. Zhang, W. Jiang, Y. Wang, Y. Yao, L. He, and K. L. Wang, "Interplay between different magnetisms in Cr-doped topological insulators," ACS Nano 7, 9205 (2013).
- ⁷⁰C.-Z. Chang, J. Zhang, M. Liu, Z. Zhang, X. Feng, K. Li, L.-L. Wang, X. Chen, X. Dai, Z. Fang, X.-L. Qi, S.-C. Zhang, Y. Wang, K. He, X.-C. Ma, and Q.-K. Xue, "Thin films of magnetically doped topological insulator with carrier-independent long-range ferromagnetic order," Adv. Mater. 7, 1065 (2013).
- ⁷¹M. Li, C.-Z. Chang, L. Wu, J. Tao, W. Zhao, M. H. W. Chan, J. S. Moodera, J. Li, and Y. Zhu, "Experimental verification of the Van Vleck nature of long-range ferromagnetic order in the vanadium-doped three-dimensional

- topological insulator Sb₂Te₃," Phys. Rev. Lett. 114, 146802 (2015).
- ⁷² W. Wang, Y. Ou, C. Liu, Y. Wang, K. He, Q.-K. Xue, and W. Wu, "Direct evidence of ferromagnetism in a quantum anomalous Hall system," Nat. Phys. 14, 791 (2018).
- ⁷³H. Li, Y. R. Song, M.-Y. Yao, F. Yang, L. Miao, F. Zhu, C. Liu, C. L. Gao, D. Qian, X. Yao, J.-F. Jia, Y. J. Shi, and D. Wu, "Carriers dependence of the magnetic properties in magnetic topological insulator Sb_{1.95-x}Bi_xCr_{0.05}Te₃," Appl. Phys. Lett. **101**, 072406 (2012).
- ⁷⁴M. G. Vergniory, M. M. Otrokov, D. Thonig, M. Hoffmann, I. V. Maznichenko, M. Geilhufe, X. Zubizarreta, S. Ostanin, A. Marmodoro, J. Henk, W. Hergert, I. Mertig, E. V. Chulkov, and A. Ernst, "Exchange interaction and its tuning in magnetic binary chalcogenides," Phys. Rev. B 89, 165202 (2014).
- ⁷⁵T. R. F. Peixoto, H. Bentmann, S. Schreyeck, M. Winnerlein, C. Seibel, H. Maaß, M. Al-Baidhani, K. Treiber, S. Schatz, S. Grauer, C. Gould, K. Brunner, A. Ernst, L. W. Molenkamp, and F. Reinert, "Impurity states in the magnetic topological insulator V:(Bi,Sb)₂Te₃," Phys. Rev. B 94, 195140 (2016).
- ⁷⁶M. Ye, T. Xu, G. Li, S. Qiao, Y. Takeda, Y. Saitoh, S.-Y. Zhu, M. Nurmamat, K. Sumida, Y. Ishida, S. Shin, and A. Kimura, "Negative Te spin polarization responsible for ferromagnetic order in the doped topological insulator V_{0.04}(Sb_{1-x}Bi_x)_{1.96}Te₃," Phys. Rev. B **99**, 144413 (2019).
- ⁷⁷A. Tcakaev, V. B. Zabolotnyy, R. J. Green, T. R. F. Peixoto, F. Stier, M. Dettbarn, S. Schreyeck, M. Winnerlein, R. C. Vidal, S. Schatz, H. B. Vasili, M. Valvidares, K. Brunner, C. Gould, H. Bentmann, F. Reinert, L. W. Molenkamp, and V. Hinkov, "Comparing magnetic ground-state properties of the V- and Cr-doped topological insulator (Bi,Sb)₂Te₃," Phys. Rev. B 101, 045127 (2020).
- ⁷⁸E. O. Lachman, A. F. Young, A. Richardella, J. Cuppens, H. R. Naren, Y. Anahory, A. Y. Meltzer, A. Kandala, S. Kempinger, Y. Myasoedov, M. E. Huber, N. Samarth, and E. Zeldov, "Visualization of superparamagnetic dynamics in magnetic topological insulators," Sci. Adv. 1, e1500740 (2015).
- ⁷⁹G. Qiu, P. Zhang, P. Deng, S. K. Chong, L. Tai, C. Eckberg, and K. L. Wang, "Mesoscopic transport of quantum anomalous Hall effect in the submicron size regime," Phys. Rev. Lett. 128, 217704 (2022).
- ⁸⁰ K. M. Fijalkowski, N. Liu, P. Mandal, S. Schreyeck, K. Brunner, C. Gould, and L. W. Molenkamp, "Macroscopic quantum tunneling of a topological ferromagnet," Adv. Sci. 10, 203165 (2023).
- ⁸¹L.-J. Zhou, R. Mei, Y.-F. Zhao, R. Zhang, D. Zhuo, Z.-J. Yan, W. Yuan, M. Kayyalha, M. H. W. Chan, C.-X. Liu, and C.-Z. Chang, "Confinement-induced chiral edge channel interaction in quantum anomalous Hall insulators," Phys. Rev. Lett. 130, 086201 (2023).
- ⁸²W. Wang, C.-Z. Chang, J. S. Moodera, and W. Wu, "Visualizing ferromagnetic domain behavior of magnetic topological insulator thin films," npj Quant. Mater. 1, 16023 (2016).
- ⁸³ K. Yasuda, M. Mogi, R. Yoshimi, A. Tsukazaki, K. S. Takahashi, M. Kawasaki, F. Kagawa, and Y. Tokura, "Quantized chiral edge conduction on domain walls of a magnetic topological insulator," Science 358, 1311 (2017).
- ⁸⁴ K. Yasuda, R. Wakatsuki, T. Morimoto, R. Yoshimi, A. Tsukazaki, K. S. Takahashi, M. Ezawa, M. Kawasaki, N. Nagaosa, and Y. Tokura, "Geometric Hall effects in topological insulator heterostructures," Nat. Phys. 12, 555 (2016).
- 85 C. Liu, Y. Zang, W. Ruan, Y. Gong, K. He, X. Ma, Q.-K. Xue, and Y. Wang, "Dimensional crossover-induced topological Hall effect in a magnetic topological insulator," Phys. Rev. Lett. 119, 176809 (2017).
- ⁸⁶J. Jiang, D. Xiao, F. Wang, J.-H. Shin, D. Andreoli, J. Zhang, R. Xiao, Y.-F. Zhao, M. Kayyalha, L. Zhang, K. Wang, J. Zang, C. Liu, N. Samarth, M. H. W. Chan, and C.-Z. Chang, "Concurrence of quantum anomalous Hall and topological Hall effects in magnetic topological insulator sandwich heterostructures," Nat. Mater. 19, 732 (2020).
- ⁸⁷K. M. Fijalkowski, M. Hartl, M. Winnerlein, P. Mandal, S. Schreyeck, K. Brunner, C. Gould, and L. W. Molenkamp, "Coexistence of surface and bulk ferromagnetism mimics skyrmion Hall effect in a topological insulator," Phys. Rev. X 10, 011012 (2020).
- ⁸⁸M. Liu, W. Wang, A. R. Richardella, A. Kandala, J. Li, A. Yazdani, N. Samarth, and N. P. Ong, "Large discrete jumps observed in the transition between Chern states in a ferromagnetic topological insulator," Sci. Adv. 2, e1600167 (2016).

- ⁸⁹M. Kawamura, R. Yoshimi, A. Tsukazaki, K. S. Takahashi, M. Kawasaki, and Y. Tokura, "Current-driven instability of the quantum anomalous Hall effect in ferromagnetic topological insulators," Phys. Rev. Lett. 119, 016803 (2017).
- ⁹⁰L. K. Rodenbach, I. T. Rosen, E. J. Fox, P. Zhang, L. Pan, K. L. Wang, M. A. Kastner, and D. Goldhaber-Gordon, "Bulk dissipation in the quantum anomalous Hall effect," APL Mater. 9, 081116 (2021).
- ⁹¹G. Lippertz, A. Bliesener, A. Uday, L. M. C. Pereira, A. A. Taskin, and Y. Ando, "Current-induced breakdown of the quantum anomalous Hall effect," Phys. Rev. B 106, 045419 (2022).
- ⁹²K. M. Fijalkowski, N. Liu, M. Klement, S. Schreyeck, K. Brunner, C. Gould, and L. W. Molenkamp, "A balanced quantum Hall resistor," Nat. Electron. 7, 438 (2024).
- ⁹³W. Li, M. Claassen, C.-Z. Chang, B. Moritz, T. Jia, C. Zhang, S. Rebec, J. J. Lee, M. Hashimoto, D.-H. Lu, R. G. Moore, J. S. Moodera, T. P. Devereaux, and Z.-X. Shen, "Origin of the low critical observing temperature of the quantum anomalous Hall effect in V-doped (Bi,Sb)₂Te₃ film," Sci. Rep. 6, 32732 (2016).
- ⁹⁴K. Yasuda, T. Morimoto, R. Yoshimi, M. Mogi, A. Tsukazaki, M. Kawamura, K. S. Takahashi, M. Kawasaki, N. Nagaosa, and Y. Tokura, "Large non-reciprocal charge transport mediated by quantum anomalous Hall edge states," Nat. Nanotechnol. 15, 831 (2020).
- ⁹⁵ K. M. Fijalkowski, N. Liu, P. Mandal, S. Schreyeck, K. Brunner, C. Gould, and L. W. Molenkamp, "Quantum anomalous Hall edge channels survive up to the Curie temperature," Nat. Commun. 12, 5599 (2021).
- ⁹⁶M. Mogi, R. Yoshimi, A. Tsukazaki, K. Yasuda, Y. Kozuka, K. S. Takahashi, M. Kawasaki, and Y. Tokura, "Magnetic modulation doping in topological insulators toward higher-temperature quantum anomalous Hall effect," Appl. Phys. Lett. 107, 182401 (2015).
- ⁹⁷M. Winnerlein, S. Schreyeck, S. Grauer, S. Rosenberger, K. M. Fi-jalkowski, C. Gould, K. Brunner, and L. W. Molenkamp, "Epitaxy and structural properties of (V,Bi,Sb)₂Te₃ layers exhibiting the quantum anomalous Hall effect," Phys. Rev. Mater. 1, 011201 (2017).
- ⁹⁸Y. Ou, C. Liu, G. Jiang, Y. Feng, D. Zhao, W. Wu, X.-X. Wang, W. Li, C. Song, L.-L. Wang, W. Wang, W. Wu, Y. Wang, K. He, X.-C. Ma, and Q.-K. Xue, "Enhancing the quantum anomalous Hall effect by magnetic codoping in a topological insulator," Adv. Mater. 30, 1703062 (2017).
- ⁹⁹X. Feng, Y. Feng, J. Wang, Y. Ou, Z. Hao, C. Liu, Z. Zhang, L. Zhang, C. Lin, J. Liao, Y. Li, L.-L. Wang, S.-H. Ji, X. Chen, X. Ma, S.-C. Zhang, Y. Wang, K. He, and Q.-K. Xue, "Thickness dependence of the quantum anomalous Hall effect in magnetic topological insulator films," Adv. Mater. 28, 6386 (2016).
- ¹⁰⁰Y.-F. Zhao, R. Zhang, Z.-T. Sun, L.-J. Zhou, D. Zhuo, Z.-J. Yan, H. Yi, K. Wang, M. H. W. Chan, C.-X. Liu, K. T. Law, and C.-Z. Chang, "3D quantum anomalous Hall effect in magnetic topological insulator trilayers of hundred-nanometer thickness," Adv. Mater. 36, 2310249 (2024).
- ¹⁰¹H. T. Yi, D. Jain, X. Yao, and S. Oh, "Enhanced quantum anomalous Hall effect with an active capping layer," Nano Lett. 23, 5673 (2023).
- ¹⁰²B. Skinner, T. Chen, and B. I. Shklovskii, "Why is the bulk resistivity of topological insulators so small?" Phys. Rev. Lett. 109, 176801 (2012).
- ¹⁰³T. Chen and B. I. Shklovskii, "Anomalously small resistivity and thermopower of strongly compensated semiconductors and topological insulators," Phys. Rev. B 87, 165119 (2013).
- ¹⁰⁴D. Nandi, B. Skinner, G. H. Lee, K.-F. Huang, K. Shain, C.-Z. Chang, Y. Ou, S.-P. Lee, J. Ward, J. S. Moodera, P. Kim, B. I. Halperin, and A. Yacoby, "Signatures of long-range-correlated disorder in the magnetotransport of ultrathin topological insulators," Phys. Rev. B 98, 214203 (2018).
- ¹⁰⁵Y. Huang and B. I. Shklovskii, "Disorder effects in topological insulator thin films," Phys. Rev. B 103, 165409 (2021).
- ¹⁰⁶ A. Park, A. Llanos, C.-I. Lu, Y. Chen, S. N. Abadi, C.-C. Chen, M. L. Teague, L. Tai, P. Zhang, K. L. Wang, and N.-C. Yeh, "Phonon and defect mediated quantum anomalous Hall insulator to metal transition in magnetically doped topological insulators," Phys. Rev. B 109, 075125 (2024).
- ¹⁰⁷J. Zhang, C.-Z. Chang, Z. Zhang, J. Wen, X. Feng, K. Li, M. Liu, K. He, L. Wang, X. Chen, Q.-K. Xue, X. Ma, and Y. Wang, "Band structure engineering in (Bi_{1-x}Sb_x)₂Te₃ ternary topological insulators," Nat. Commun. 2, 574 (2011).
- ¹⁰⁸A. Thenapparambil, G. E. dos Santos, C.-A. Li, M. Abdelghany, W. Beugeling, H. Buhmann, C. Gould, S.-B. Zhang, B. Trauzettel, and

- L. W. Molenkamp, "Fluctuations in planar magnetotransport due to tilted Dirac cones in topological materials," Nano Lett. 23, 6914 (2023).
- ¹⁰⁹C. Fuchs, S. Shamim, P. Shekhar, L. Fürst, J. Kleinlein, J. I. Väyrynen, H. Buhmann, and L. W. Molenkamp, "Kondo interaction of quantum spin Hall edge channels with charge puddles," Phys. Rev. B 108, 205302 (2023).
- ¹¹⁰J. P. Faurie and A. Million, "Molecular beam epitaxy of II–VI compounds: Cd_xHg_{1-x}Te," J. Cryst. Growth **54**, 582 (1981).
- ¹¹¹W. D. Lawson, S. Nielsen, E. H. Putley, and A. S. Young, "Preparation and properties of HgTe and mixed crystals of HgTe-CdTe," J. Phys. Chem. Solids 9, 325 (1959).
- ¹¹²I. T. Rosen, M. P. Andersen, L. K. Rodenbach, L. Tai, P. Zhang, K. L. Wang, M. A. Kastner, and D. Goldhaber-Gordon, "Measured potential profile in a quantum anomalous Hall system suggests bulk-dominated current flow," Phys. Rev. Lett. 129, 246602 (2022).
- ¹¹³G. M. Ferguson, R. Xiao, A. R. Richardella, D. Low, N. Samarth, and K. C. Nowack, "Direct visualization of electronic transport in a quantum anomalous Hall insulator," Nat. Mater. 22, 1100 (2023).
- ¹¹⁴K. M. Fijalkowski and C. Gould, "Quantization breakdown protection for semiconductors and in perticular topological insulators," European patent filing EP23162996.5 (2023).
- ¹¹⁵R. Ribeiro-Palau, F. Lafont, J. Brun-Picard, D. Kazazis, A. Michon, F. Cheynis, O. Couturaud, C. Consejo, B. Jouault, W. Poirier, and F. Schopfer, "Quantum Hall resistance standard in graphene devices under relaxed experimental conditions," Nat. Nanotechnol. 10, 965 (2015).
- ¹¹⁶A. A. Taskin, S. Sasaki, K. Segawa, and Y. Ando, "Manifestation of topological protection in transport properties of epitaxial Bi₂Se₃ thin films," Phys. Rev. Lett. **109**, 066803 (2012).
- ¹¹⁷J. J. Lee, F. T. Schmitt, R. G. Moore, I. M. Vishik, Y. Ma, and Z. X. Shen, "Intrinsic ultrathin topological insulators grown via molecular beam epitaxy characterized by in-situ angle resolved photoemission spectroscopy," Appl. Phys. Lett. 101, 013118 (2012).
- ¹¹⁸N. Bansal, Y. S. Kim, M. Brahlek, E. Edrey, and S. Oh, "Thickness-independent transport channels in topological insulator Bi₂Se₃ thin films," Phys. Rev. Lett. **109**, 116804 (2012).
- ¹¹⁹S. E. Harrison, S. Li, Y. Huo, B. Zhou, Y. L. Chen, and J. S. Harris, "Two-step growth of high quality Bi₂Te₃ thin films on Al₂O₃ (0001) by molecular beam epitaxy," Appl. Phys. Lett. **102**, 171906 (2013).
- ¹²⁰Y. Zhao, C.-Z. Chang, Y. Jiang, A. DaSilva, Y. Sun, H. Wang, Y. Xing, Y. Wang, K. He, X. Ma, Q.-K. X. Xue, and J. Wang, "Demonstration of surface transport in a hybrid Bi₂Se₃/Bi₂Te₃ heterostructure," Sci. Rep. 3, 3060 (2013).
- ¹²¹J. Chen, H. J. Qin, F. Yang, J. Liu, T. Guan, F. M. Qu, G. H. Zhang, J. R. Shi, X. C. Xie, C. L. Yang, K. H. Wu, Y. Q. Li, and L. Lu, "Gate-voltage control of chemical potential and weak antilocalization in Bi₂Se₃," Phys. Rev. Lett. 105, 176602 (2010).
- ¹²²G. Zhang, H. Qin, J. Chen, X. He, L. Lu, Y. Li, and K. Wu, "Growth of topological insulator Bi₂Se₃ thin films on SrTiO₃ with large tunability in chemical potential," Adv. Funct. Mater. 21, 2351 (2011).
- ¹²³ A. Richardella, D. M. Zhang, J. S. Lee, A. Koser, D. W. Rench, A. L. Yeats, B. B. Buckley, D. D. Awschalom, and N. Samarth, "Coherent heteroepitaxy of Bi₂Se₃ on GaAs (111)B," Appl. Phys. Lett. 97, 262104 (2010).
- ¹²⁴Z. Chen, T. A. Garcia, J. De Jesus, L. Zhao, H. Deng, J. Secor, M. Begliar-bekov, L. Krusin-Elbaum, and M. C. Tamargo, "Molecular beam epitaxial growth and properties of Bi₂Se₃ topological insulator layers on different substrate surfaces," J. Electron. Mater. 43, 909 (2014).
- ¹²⁵M. Eddrief, P. Atkinson, V. Etgens, and B. Jusserand, "Low-temperature raman fingerprints for few-quintuple layer topological insulator Bi₂Se₃ films epitaxied on GaAs," Nanotechnology 25, 245701 (2014).
- ¹²⁶X. Liu, D. J. Smith, J. Fan, Y. Zhang, H. Cao, Y. P. Chen, B. J. Kirby, N. Sun, S. T. Ruggiero, J. Leiner, R. E. Pimpinella, J. Hagmann, K. Tivakornsasithorn, M. Dobrowolska, and J. K. Furdyna, "Topological insulators Bi₂Te₃ and Bi₂Se₃ grown by MBE on (001) GaAs substrates," AIP Conf. Proc. 1416, 105 (2011).
- ¹²⁷T. Guillet, A. Marty, C. Beigne, C. Vergnaud, M.-T. Dau, P. Noel, J. Frigerio, G. Isella, and M. Jamet, "Magnetotransport in Bi₂Se₃ thin films epitaxially grown on Ge(111)," AIP Adv. 8, 115125 (2018).
- ¹²⁸S. Kim, S. Lee, J. Woo, and G. Lee, "Growth of Bi₂Se₃ topological insulator thin film on Ge(111) substrate," Appl. Surf. Sci. 432, 152 (2018).

- ¹²⁹G. Zhang, H. Qin, J. Teng, J. Guo, Q. Guo, X. Dai, Z. Fang, and K. Wu, "Quintuple-layer epitaxy of thin films of topological insulator Bi₂Se₃," Appl. Phys. Lett. 95, 053114 (2009).
- ¹³⁰ Y.-Y. Li, G. Wang, X.-G. Zhu, M.-H. Liu, C. Ye, X. Chen, Y.-Y. Wang, K. He, L.-L. Wang, X.-C. Ma, H.-J. Zhang, X. Dai, Z. Fang, X.-C. Xie, Y. Liu, X.-L. Qi, J.-F. Jia, S.-C. Zhang, and Q.-K. Xue, "Intrinsic topological insulator Bi₂Te₃ thin films on Si and their thickness limit," Adv. Mater. 22, 4002 (2010).
- ¹³¹L. He, F. Xiu, Y. Wang, A. V. Fedorov, G. Huang, X. Kou, M. Lang, W. P. Beyermann, J. Zou, and K. L. Wang, "Epitaxial growth of Bi₂Se₃ topological insulator thin films on Si (111)," J. Appl. Phys. 109, 103702 (2011).
- ¹³²J. Krumrain, G. Mussler, S. Borisova, T. Stoica, L. Plucinski, C. Schneider, and D. Grützmacher, "MBE growth optimization of topological insulator Bi₂Te₃ films," J. Cryst. Growth 324, 115 (2011).
- ¹³³ X. Liu, D. J. Smith, J. Fan, Y.-H. Zhang, H. Cao, Y. P. Chen, J. Leiner, B. J. Kirby, M. Dobrowolska, and J. K. Furdyna, "Structural properties of Bi₂Te₃ and Bi₂Se₃ topological insulators grown by molecular beam epitaxy on GaAs(001) substrates," Appl. Phys. Lett. 99, 171903 (2011).
- ¹³⁴X. Liu, D. J. Smith, H. Cao, Y. P. Chen, J. Fan, Y.-H. Zhang, R. E. Pimpinella, M. Dobrowolska, and J. K. Furdyna, "Characterization of Bi₂Te₃ and Bi₂Se₃ topological insulators grown by MBE on (001) GaAs substrates," J. Vac. Sci. Technol. B 30, 02B103 (2011).
- ¹³⁵X. F. Kou, L. He, F. X. Xiu, M. R. Lang, Z. M. Liao, Y. Wang, A. V. Fedorov, X. X. Yu, J. S. Tang, G. Huang, X. W. Jiang, J. F. Zhu, J. Zou, and K. L. Wang, "Epitaxial growth of high mobility Bi₂Se₃ thin films on CdS," Appl. Phys. Lett. 98, 242102 (2011).
- ¹³⁶Y. Zhang, K. He, C.-Z. Chang, C.-L. Song, L.-L. Wang, X. Chen, J.-F. Jia, Z. Fang, X. Dai, W.-Y. Shan, S.-Q. Shen, Q. Niu, X.-L. Qi, S.-C. Zhang, X.-C. Ma, and Q.-K. Xue, "Crossover of the three-dimensional topological insulator Bi₂Se₃ to the two-dimensional limit," Nat. Phys. 6, 584 (2010).
- ¹³⁷L. He, X. Kou, and K. L. Wang, "Review of 3D topological insulator thinfilm growth by molecular beam epitaxy and potential applications," Phys. Status Solidi RRL 7, 50 (2013).
- ¹³⁸A. Koma, K. Sunouchi, and T. Miyajima, "Fabrication of ultrathin heterostructures with van der Waals epitaxy," J. Vac. Sci. Technol. B 3, 724 (1985).
- ¹³⁹A. Koma, "Van der Waals epitaxy a new epitaxial growth method for a highly lattice-mismatched system," Thin Solid Films 216, 72 (1992).
- ¹⁴⁰F. Bonell, M. G. Cuxart, K. Song, R. Robles, P. Ordejon, S. Roche, A. Mugarza, and S. O. Valenzuela, "Growth of twin-free and low-doped topological insulators on BaF₂(111)," Cryst. Growth Des. 17, 4655 (2017).
- ¹⁴¹N. Bansal, N. Koirala, M. Brahlek, M.-G. Han, Y. Zhu, Y. Cao, J. Waugh, D. S. Dessau, and S. Oh, "Robust topological surface states of Bi₂Se₃ thin films on amorphous SiO₂/Si substrate and a large ambipolar gating effect," Appl. Phys. Lett. **104**, 241606 (2014).
- ¹⁴²D. S. H. Liu, M. Hilse, and R. Engel-Herbert, "Sticking coefficients of selenium and tellurium," J. Vac. Sci. Technol. A 39, 023413 (2021).
- ¹⁴³L. Zhang, R. Hammond, M. Dolev, M. Liu, A. Palevski, and A. Kapitulnik, "High quality ultrathin Bi₂Se₃ films on CaF₂ and CaF₂/Si by molecular beam epitaxy with a radio frequency cracker cell," Appl. Phys. Lett. 101, 153105 (2012).
- ¹⁴⁴R. Yoshimi, A. Tsukazaki, Y. Kozuka, J. Falson, K. S. Takahashi, J. G. Checkelsky, N. Nagaosa, M. Kawasaki, and Y. Tokura, "Quantum Hall effect on top and bottom surface states of topological insulator (Bi_{1-x}Sb_x)₂Te₃ films," Nat. Commun. 6, 6627 (2015).
- ¹⁴⁵J. Liu and T. Hesjedal, "Magnetic topological insulator heterostructures: a review," Adv. Mater. 35, 2102427 (2023).
- ¹⁴⁶J. Yuan, W. Ma, L. Zhang, Y. Lu, M. Zhao, H. Guo, J. Zhao, W. Yu, Y. Zhang, K. Zhang, H. Y. Hoh, X. Li, K. P. Loh, S. Li, C.-W. Qiu, and Q. Bao, "Infrared nanoimaging reveals the surface metallic plasmons in topological insulator," ACS Photonics 4, 3055 (2017).
- ¹⁴⁷S. E. Harrison, L. J. Collins-McIntyre, S. Li, A. A. Baker, L. R. Shelford, Y. Huo, A. Pushp, S. S. P. Parkin, J. S. Harris, E. Arenholz, G. van der Laan, and T. Hesjedal, "Study of Gd-doped Bi₂Te₃ thin films: molecular beam epitaxy growth and magnetic properties," J. Appl. Phys. 115, 023904 (2014).
- ¹⁴⁸S. E. Harrison, L. J. Collins-McIntyre, P. Schönherr, A. Vailionis, V. Srot, P. A. van Aken, A. Kellock, A. Pushp, S. S. Parkin, J. Harris, *et al.*, "Massive Dirac fermion observed in lanthanide-doped topological insulator thin

- films," Sci. Rep. 5, 15767 (2015).
- ¹⁴⁹P. Ngabonziza, R. Heimbuch, N. de Jong, R. A. Klaassen, M. P. Stehno, M. Snelder, A. Solmaz, S. V. Ramankutty, E. Frantzeskakis, E. van Heumen, G. Koster, M. S. Golden, H. J. W. Zandvliet, and A. Brinkman, "In situ spectroscopy of intrinsic Bi₂Te₃ topological insulator thin films and impact of extrinsic defects," Phys. Rev. B 92, 035405 (2015).
- ¹⁵⁰B. Leedahl, D. W. Boukhvalov, E. Z. Kurmaev, A. Kukharenko, I. S. Zhid-kov, N. V. Gavrilov, S. O. Cholakh, P. H. Le, C. W. Luo, and A. Moewes, "Bulk vs. surface structure of 3*d* metal impurities in topological insulator Bi₂Te₃," Sci. Rep. 7, 5758 (2017).
- ¹⁵¹D. D. dos Reis, L. Barreto, M. Bianchi, G. A. S. Ribeiro, E. A. Soares, W. S. e Silva, V. E. de Carvalho, J. Rawle, M. Hoesch, C. Nicklin, W. P. Fernandes, J. Mi, B. B. Iversen, and P. Hofmann, "Surface structure of Bi₂Se₃(111) determined by low-energy electron diffraction and surface x-ray diffraction," Phys. Rev. B 88, 041404 (2013).
- ¹⁵²L. J. Collins-McIntyre, S. E. Harrison, P. Schönherr, N.-J. Steinke, C. J. Kinane, T. R. Charlton, D. Alba-Veneroa, A. Pushp, A. J. Kellock, S. S. P. Parkin, J. S. Harris, S. Langridge, G. van der Laan, and T. Hesjedal, "Magnetic ordering in Cr-doped Bi₂Se₃ thin films," EPL 107, 57009 (2014).
- ¹⁵³P. P. J. Haazen, J.-B. Laloë, T. J. Nummy, H. J. M. Swagten, P. Jarillo-Herrero, D. Heiman, and J. S. Moodera, "Ferromagnetism in thin-film Cr-doped topological insulator Bi₂Se₃," Appl. Phys. Lett. **100**, 082404 (2012).
- ¹⁵⁴S. M. Mostafavi Kashani, V. G. Dubrovskii, T. Baumbach, and U. Pietsch, "In situ monitoring of MBE growth of a single self-catalyzed GaAs nanowire by x-ray diffraction," J. Phys. Chem. C 125, 22724 (2021).
- ¹⁵⁵Y. Liu, M. Weinert, and L. Li, "Spiral growth without dislocations: molecular beam epitaxy of the topological insulator Bi₂Se₃ on epitaxial graphene/SiC(0001)," Phys. Rev. Lett. 108, 115501 (2012).
- ¹⁵⁶A. Karma and M. Plapp, "Spiral surface growth without desorption," Phys. Rev. Lett. 81, 4444 (1998).
- ¹⁵⁷S. E. Harrison, L. J. Collins-McIntyre, S. L. Zhang, A. A. Baker, A. I. Figueroa, A. J. Kellock, A. Pushp, Y. L. Chen, S. S. P. Parkin, J. S. Harris, G. van der Laan, and T. Hesjedal, "Study of Ho-doped Bi₂Te₃ topological insulator thin films," Appl. Phys. Lett. 107, 182406 (2015).
- ¹⁵⁸A. I. Figueroa, G. van der Laan, L. J. Collins-McIntyre, G. Cibin, A. J. Dent, and T. Hesjedal, "Local structure and bonding of transition metal dopants in Bi₂Se₃ topological insulator thin films," J. Phys. Chem. C 119, 17344 (2015).
- ¹⁵⁹Z. Liu, X. Wei, J. Wang, H. Pan, F. Ji, F. Xi, J. Zhang, T. Hu, S. Zhang, Z. Jiang, W. Wen, Y. Huang, M. Ye, Z. Yang, and S. Qiao, "Local structures around 3d metal dopants in topological insulator Bi₂Se₃ studied by EXAFS measurements," Phys. Rev. B 90, 094107 (2014).
- ¹⁶⁰H. Yang, A. Liang, C. Chen, C. Zhang, N. B. Schroeter, and Y. Chen, "Visualizing electronic structures of quantum materials by angle-resolved photoemission spectroscopy," Nat. Rev. Mater. 3, 341 (2018).
- ¹⁶¹Y. Xia, D. Qian, D. Hsieh, L. Wray, A. Pal, H. Lin, A. Bansil, D. Grauer, Y. S. Hor, R. J. Cava, and M. Z. Hasan, "Observation of a large-gap topological-insulator class with a single dirac cone on the surface," Nat. Phys. 5, 398 (2009).
- ¹⁶²Y. L. Chen, J. G. Analytis, J.-H. Chu, Z. K. Liu, S.-K. Mo, X. L. Qi, H. J. Zhang, D. H. Lu, X. Dai, Z. Fang, S. C. Zhang, I. R. Fisher, Z. Hussain, and Z.-X. Shen, "Experimental realization of a three-dimensional topological insulator Bi₂Te₃," Science 325, 178 (2009).
- ¹⁶³Y. L. Chen, J.-H. Chu, J. G. Analytis, Z. K. Liu, K. Igarashi, H.-H. Kuo, X. L. Qi, S. K. Mo, R. G. Moore, D. H. Lu, M. Hashimoto, T. Sasagawa, S. C. Zhang, I. R. Fisher, Z. Hussain, and Z. X. Shen, "Massive Dirac fermion on the surface of a magnetically doped topological insulator," Science 329, 659 (2010).
- ¹⁶⁴C.-Y. Lim, S. Kim, S. W. Jung, J. Hwang, and Y. Kim, "Recent technical advancements in ARPES: unveiling quantum materials," Curr. Appl. Phys. 60, 43 (2024).
- ¹⁶⁵ J. A. Alexander-Webber, J. Huang, J. Beilsten-Edmands, P. Čermák, Č Drašar, R. J. Nicholas, and A. I. Coldea, "Multi-band magnetotransport in exfoliated thin films of Cu_xBi₂Se₃," J. Phys.: Condens. Matter 30, 155302 (2018).
- ¹⁶⁶J. Huang, J. A. Alexander-Webber, A. M. R. Baker, T. J. B. M. Janssen, A. Tzalenchuk, V. Antonov, T. Yager, S. Lara-Avila, S. Kubatkin, R. Yakimova, and R. J. Nicholas, "Physics of a disordered Dirac point in epitaxial graphene from temperature-dependent magnetotransport measurements,"

- Phys. Rev. B 92, 075407 (2015).
- ¹⁶⁷H. J. Joyce, J. L. Boland, C. L. Davies, S. A. Baig, and M. B. Johnston, "A review of the electrical properties of semiconductor nanowires: insights gained from terahertz conductivity spectroscopy," Semicond. Sci. Technol. 31, 103003 (2016).
- ¹⁶⁸S. Sim, M. Brahlek, N. Koirala, S. Cha, S. Oh, and H. Choi, "Ultrafast terahertz dynamics of hot Dirac-electron surface scattering in the topological insulator Bi₂Se₃," Phys. Rev. B 89, 165137 (2014).
- ¹⁶⁹P. H. Le, P.-T. Liu, C. W. Luo, J.-Y. Lin, and K. H. Wu, "Thickness-dependent magnetotransport properties and terahertz response of topological insulator Bi₂Te₃ thin films," J. Alloys Compd. 692, 972 (2017).
- ¹⁷⁰L. Ding, M. Wu, S. Zhou, L. Zhu, H. Wen, X. Cheng, and W. Xu, "Study of the surface and bulk states of Bi₂Te₃ topological insulators using terahertz time-domain spectroscopy," Phys. Status Solidi RRL 17, 2300008 (2023).
- ¹⁷¹V. S. Kamboj, A. Singh, T. Ferrus, H. E. Beere, L. B. Duffy, T. Hesjedal, C. H. W. Barnes, and D. A. Ritchie, "Probing the topological surface state in Bi₂Se₃ thin films using temperature-dependent terahertz spectroscopy," ACS Photonics 4, 2711 (2017).
- ¹⁷²J. A. Sobota, S. Yang, J. G. Analytis, Y. L. Chen, I. R. Fisher, P. S. Kirchmann, and Z.-X. Shen, "Ultrafast optical excitation of a persistent surface-state population in the topological insulator Bi₂Se₃," Phys. Rev. Lett. 108, 117403 (2012).
- ¹⁷³A. De, T. K. Bhowmick, and R. K. Lake, "Anomalous magneto-optical effects in an antiferromagnet-topological-insulator heterostructure," Phys. Rev. Appl. 16, 014043 (2021).
- ¹⁷⁴F. Mooshammer, F. Sandner, M. A. Huber, M. Zizlsperger, H. Weigand, M. Plankl, C. Weyrich, M. Lanius, J. Kampmeier, G. Mussler, D. Grützmacher, J. L. Boland, T. L. Cocker, and R. Huber, "Nanoscale near-field tomography of surface states on (Bi_{0.5}Sb_{0.5})₂Te₃," Nano Lett. 18, 7515 (2018).
- ¹⁷⁵E. A. A. Pogna, L. Viti, A. Politano, M. Brambilla, G. Scamarcio, and M. S. Vitiello, "Mapping propagation of collective modes in Bi₂Se₃ and Bi₂Te_{2.2}Se_{0.8} topological insulators by near-field terahertz nanoscopy," Nat. Commun. 12, 6672 (2021).
- ¹⁷⁶D. Johnson, T. Vincent, X. Liu, B. Gholizadeh, P. Schöenherr, T. Hesjedal, O. Kazakova, N. Huang, and J. Boland, "Scattering-type near-field optical microscopy characterization of topological insulator Bi₂Te₃ nanowires," in 2023 48th International Conference on Infrared, Millimeter, and Terahertz Waves (IRMMW-THz) (2023) p. 1.
- ¹⁷⁷G. Romagnoli, E. Marchiori, K. Bagani, and M. Poggio, "Fabrication of Nb and MoGe SQUID-on-tip probes by magnetron sputtering," Appl. Phys. Lett. 122, 192603 (2023).
- ¹⁷⁸E. Persky, I. Sochnikov, and B. Kalisky, "Studying quantum materials with scanning SQUID microscopy," Annu. Rev. Condens. Matter Phys. 13, 385 (2022).
- ¹⁷⁹T. Wang, C. Wu, M. Mogi, M. Kawamura, Y. Tokura, Z.-X. Shen, Y.-Z. You, and M. T. Allen, "Probing the edge states of Chern insulators using microwave impedance microscopy," Phys. Rev. B 108, 235432 (2023).
- ¹⁸⁰S. Kim, J. Schwenk, D. Walkup, Y. Zeng, F. Ghahari, S. T. Le, M. R. Slot, J. Berwanger, S. R. Blankenship, K. Watanabe, F. J. Giessibl, N. B. Zhitenev, C. R. Dean, and J. A. Stroscio, "Edge channels of brokensymmetry quantum Hall states in graphene visualized by atomic force microscopy," Nat. Commun. 12, 2852 (2021).
- ¹⁸¹F. Keilmann and R. Hillenbrand, "Near-field microscopy by elastic light scattering from a tip," Philos. Trans. R. Soc. A 362, 787 (2004).
- ¹⁸²G. Dai, Z. Yang, G. Geng, M. Li, T. Chang, D. Wei, C. Du, H.-L. Cui, and H. Wang, "Signal detection techniques for scattering-type scanning near-field optical microscopy," Appl. Spectrosc. Rev. 53, 806 (2018).
- ¹⁸³J. Lloyd-Hughes, P. M. Oppeneer, T. P. dos Santos, A. Schleife, S. Meng, M. A. Sentef, M. Ruggenthaler, A. Rubio, I. Radu, M. Murnane, X. Shi, H. Kapteyn, B. Stadtmüller, K. M. Dani, F. H. da Jornada, E. Prinz, M. Aeschlimann, R. L. Milot, M. Burdanova, J. Boland, T. Cocker, and F. Hegmann, "The 2021 ultrafast spectroscopic probes of condensed matter roadmap," J. Phys.: Condens. Matter 33, 353001 (2021).
- ¹⁸⁴X. Chen, D. Hu, R. Mescall, G. You, D. N. Basov, Q. Dai, and M. Liu, "Modern scattering-type scanning near-field optical microscopy for advanced material research," Adv. Mater. 31, 1804774 (2019).
- ¹⁸⁵T. Taubner, F. Keilmann, and R. Hillenbrand, "Nanoscale-resolved subsurface imaging by scattering-type near-field optical microscopy," Opt. Ex-

- press 13, 8893 (2005).
- ¹⁸⁶B. Kusnetz, J. Belhassen, D. E. Tranca, S. G. Stanciu, S.-R. Anton, Z. Zalevsky, G. A. Stanciu, and A. Karsenty, "Generic arrays of surface-positioned and shallow-buried gold multi-shapes as reference samples to benchmark near-field microscopes. Part 1: applications in s-SNOM depth imaging," Results Phys. 56, 107318 (2024).
- ¹⁸⁷K. Moon, H. Park, J. Kim, Y. Do, S. Lee, G. Lee, H. Kang, and H. Han, "Subsurface nanoimaging by broadband terahertz pulse near-field microscopy," Nano Lett. 15, 549 (2015).
- ¹⁸⁸ A. Cvitkovic, N. Ocelic, and R. Hillenbrand, "Analytical model for quantitative prediction of material contrasts in scattering-type near-field optical microscopy," Opt. Express 15, 8550 (2007).
- ¹⁸⁹B. Hauer, A. P. Engelhardt, and T. Taubner, "Quasi-analytical model for scattering infrared near-field microscopy on layered systems," Opt. Express 20, 13173 (2012).
- ¹⁹⁰A. S. McLeod, P. Kelly, M. D. Goldflam, Z. Gainsforth, A. J. Westphal, G. Dominguez, M. H. Thiemens, M. M. Fogler, and D. N. Basov, "Model for quantitative tip-enhanced spectroscopy and the extraction of nanoscale-resolved optical constants," Phys. Rev. B 90, 085136 (2014).
- ¹⁹¹L. Mester, A. A. Govyadinov, S. Chen, M. Goikoetxea, and R. Hillenbrand, "Subsurface chemical nanoidentification by nano-FTIR spectroscopy," Nat. Commun. 11, 3359 (2020).
- ¹⁹²T. Vincent, X. Liu, D. Johnson, L. Mester, N. Huang, O. Kazakova, R. Hillenbrand, and J. L. Boland, "snompy: a package for modelling scattering-type scanning near-field optical microscopy," arXiv: 2405.20948 (2024).
- ¹⁹³C. Kastl, M. Stallhofer, D. Schuh, W. Wegscheider, and A. W. Holleitner, "Optoelectronic transport through quantum Hall edge states," New J. Phys. 17, 023007 (2015).
- ¹⁹⁴H. Ito, K. Furuya, Y. Shibata, S. Kashiwaya, M. Yamaguchi, T. Akazaki, H. Tamura, Y. Ootuka, and S. Nomura, "Near-field optical mapping of quantum Hall edge states," Phys. Rev. Lett. 107, 256803 (2011).
- ¹⁹⁵S. Mamyouda, H. Ito, Y. Shibata, S. Kashiwaya, M. Yamaguchi, T. Akazaki, H. Tamura, Y. Ootuka, and S. Nomura, "Circularly polarized near-field optical mapping of spin-resolved quantum Hall chiral edge states," Nano Lett. 15, 2417 (2015).
- ¹⁹⁶D. Hu, C. Luo, L. Kang, M. Liu, and Q. Dai, "Few-layer hexagonal boron nitride as a shield of brittle materials for cryogenic s-SNOM exploration of phonon polaritons," Appl. Phys. Lett. 120, 161101 (2022).
- ¹⁹⁷R. H. J. Kim, J.-M. Park, S. J. Haeuser, L. Luo, and J. Wang, "A sub-2 Kelvin cryogenic magneto-terahertz scattering-type scanning near-field optical microscope (cm-THz-sSNOM)," Rev. Sci. Instrum. 94, 043702 (2023).
- 198 A. Leitenstorfer, A. S. Moskalenko, T. Kampfrath, J. Kono, E. Castro-Camus, K. Peng, N. Qureshi, D. Turchinovich, K. Tanaka, A. G. Markelz, M. Havenith, C. Hough, H. J. Joyce, W. J. Padilla, B. Zhou, K.-Y. Kim, X.-C. Zhang, P. U. Jepsen, S. Dhillon, M. Vitiello, E. Linfield, A. G. Davies, M. C. Hoffmann, R. Lewis, M. Tonouchi, P. Klarskov, T. S. Seifert, Y. A. Gerasimenko, D. Mihailovic, R. Huber, J. L. Boland, O. Mitrofanov, P. Dean, B. N. Ellison, P. G. Huggard, S. P. Rea, C. Walker, D. T. Leisawitz, J. R. Gao, C. Li, Q. Chen, G. Valušis, V. P. Wallace, E. Pickwell-MacPherson, X. Shang, J. Hesler, N. Ridler, C. C. Renaud, I. Kallfass, T. Nagatsuma, J. A. Zeitler, D. Arnone, M. B. Johnston, and J. Cunningham, "The 2023 terahertz science and technology roadmap," J. Phys. D: Appl. Phys. 56, 223001 (2023).
- ¹⁹⁹ A. A. Govyadinov, I. Amenabar, F. Huth, P. S. Carney, and R. Hillenbrand, "Quantitative measurement of local infrared absorption and dielectric function with tip-enhanced near-field microscopy," J. Phys. Chem. Lett. 4, 1526 (2013).
- ²⁰⁰X. Chen, R. Ren, and M. Liu, "Validity of machine learning in the quantitative analysis of complex scanning near-field optical microscopy signals using simulated data," Phys. Rev. Appl. 15, 014001 (2021).
- ²⁰¹J. Brun-Picard, S. Djordjevic, D. Leprat, F. Schopfer, and W. Poirier, "Practical quantum realization of the ampere from the elementary charge," Phys. Rev. X 6, 041051 (2016).
- ²⁰²L. K. Rodenbach, N. T. M. Tran, J. M. Underwood, A. R. Panna, M. P. Andersen, Z. S. Barcikowski, S. U. Payagala, P. Zhang, L. Tai, K. L. Wang, R. E. Elmquist, D. G. Jarrett, D. B. Newell, A. F. Rigosi, and D. Goldhaber-Gordon, "Realization of the quantum ampere using the quantum anomalous Hall and Josephson effects," arXiv:2308.00200 (2023).

- ²⁰³W. Poirier and F. Schopfer, "Resistance metrology based on the quantum Hall effect," Eur. Phys. J.: Spec. Top. 172, 207 (2009).
- ²⁰⁴B. Jeckelmann and B. Jeanneret, "The quantum Hall effect as an electrical resistance standard," Rep. Prog. Phys. 64, 1603 (2001).
- ²⁰⁵F. Delahaye and B. Jeckelmann, "Revised technical guidelines for reliable dc measurements of the quantized Hall resistance," Metrologia 40, 217 (2003).
- ²⁰⁶"BIPM.EM-K12," BIPM Key Comparison Database. Expanded relative uncertainties for resistance calibration services of more than 10 institutes are within 3 to 100 parts in 10⁹.
- ²⁰⁷D. Drung, M. Götz, E. Pesel, J.-H. Storm, C. Aßmann, M. Peters, and T. Schurig, "Improving the stability of cryogenic current comparator setups," Supercond. Sci. Technol. 22, 114004 (2009).
- ²⁰⁸M. Götz, D. Drung, E. Pesel, H.-J. Barthelmess, C. Hinnrichs, C. Assmann, M. Peters, H. Scherer, B. Schumacher, and T. Schurig, "Improved cryogenic current comparator setup with digital current sources," IEEE Trans. Instrum. Meas. 58, 1176 (2009).
- ²⁰⁹D. Drung and J.-H. Storm, "Ultralow-noise chopper amplifier with low input charge injection," IEEE Trans. Instrum. Meas. 60, 2347 (2011).
- ²¹⁰D. Drung, M. Götz, E. Pesel, and H. Scherer, "Improving the traceable measurement and generation of small direct currents," IEEE Trans. Instrum. Meas. 64, 3021 (2015).
- ²¹¹D. K. Patel, K. M. Fijalkowski, M. Kruskopf, N. Liu, M. Götz, E. Pesel, M. Jaime, M. Klement, S. Schreyeck, K. Brunner, C. Gould, L. W. Molenkamp, and H. Scherer, "Temperature dependence of a quantum resistance standard at zero external magnetic field," in *IMEKO 2024 XXIV World Congress* (Hamburg, Germany, 2024).
- ²¹²B. Jeckelmann, A. Rufenacht, B. Jeanneret, F. Overney, K. Pierz, A. von Campenhausen, and G. Hein, "Optimization of QHE-devices for metrological applications," IEEE Trans. Instrum. Meas. 50, 218 (2001).
- ²¹³F. Delahaye, "Series and parallel connection of multiterminal quantum Hall-effect devices," J. Appl. Phys. **73**, 7914 (1993).
- ²¹⁴M. Kruskopf, A. F. Rigosi, A. R. Panna, D. K. Patel, H. Jin, M. Marzano, M. Berilla, D. B. Newell, and R. E. Elmquist, "Two-terminal and multi-

- terminal designs for next-generation quantized Hall resistance standards: contact material and geometry," IEEE Trans. Electron Devices **66**, 3973 (2019)
- ²¹⁵M. E. Cage, B. F. Field, R. F. Dziuba, S. M. Girvin, A. C. Gossard, and D. C. Tsui, "Temperature dependence of the quantum Hall resistance," Phys. Rev. B 30, 2286 (1984).
- ²¹⁶M. D'Iorio and B. Wood, "Temperature dependence of the quantum hall resistance," Surface Science 170, 233 (1986).
- ²¹⁷F. Delahaye, D. Dominguez, F. Alexandre, J. P. Andre, J. P. Hirtz, and M. Razeghi, "Precise quantized Hall resistance measurements in GaAs/Al_xGa_{1-x}As and In_xGa_{1-x}As/InP heterostructures," Metrologia 22, 103 (1986)
- ²¹⁸K. Yoshihiro, J. Kinoshita, K. Inagaki, C. Yamanouchi, T. Endo, Y. Murayama, M. Koyanagi, A. Yagi, J. Wakabayashi, and S. Kawaji, "Quantum Hall effect in silicon metal-oxide-semiconductor inversion layers: experimental conditions for determination of h/e^2 ," Phys. Rev. B **33**, 6874 (1986).
- ²¹⁹M. Furlan, "Electronic transport and the localization length in the quantum Hall effect," Phys. Rev. B 57, 14818 (1998).
- ²²⁰A. Hartland, "The quantum Hall effect and resistance standards," Metrologia 29, 175 (1992).
- ²²¹F. Schopfer and W. Poirier, "Quantum resistance standard accuracy close to the zero-dissipation state," J. Appl. Phys. **114**, 064508 (2013).
- ²²²F. Lafont, R. Ribeiro-Palau, D. Kazazis, A. Michon, O. Couturaud, C. Consejo, T. Chassagne, M. Zielinski, M. Portail, B. Jouault, et al., "Quantum Hall resistance standards from graphene grown by chemical vapour deposition on silicon carbide," Nat. Commun. 6, 6806 (2015).
- 223 T. Hesjedal, "Rare earth doping of topological insulators: a brief review of thin film and heterostructure systems," Phys. Status Solidi A, 216, 1800726 (2019).
- 224 European Joint Research Project, "23FUN07 QuAHMET (Quantum Anomalous Hall Effect Materials and Devices for Metrology)," Project website: https://sites.google.com/inrim.it/quahmet.